Design Study for Optimum Multivariable Control System for Wind Tunnel Regulation

دراسة تصميم أفضل نظم التحكم ذات المتغيرات المتعددة للنفق الهوائي

By

Ashraf Hussein Ashour

Student ID number: 120171

Dissertation submitted to the British University in Dubai in partial fulfilment of the of MSc in Systems Engineering

Faculty of Engineering

Dissertation Supervisor

Professor Robert Whalley

August-2016

ABSTRACT

This Dissertation investigates the design of a multivariable control system for a wind tunnel to obtain the optimum control strategy in order to minimize energy dissipation, noise and cost which improve the quality and integrity of the wind tunnel test measurements.

First the research is focused on identifying how a wind tunnel work with brief information about its components and types. Then the least effort control technique will be applied and discussed. Also study includes a controller designed by the Nyquist Array method and other control strategies.

Plots of step response, disturbance suppression and transient recovery for both techniques will be presented with their block diagrams.

The dissertation concludes with a comparison of the control methods used, based on the performance and energy dissipation.

خلاصة البحث

يتضمن البحث دراسة تصميم نظام تحكم ذو متغيرات متعددة للنفق الهوائي بإستخدام ألية جديدة تتميز بإستهلاك اقل للطاقة و تقليل تأثير العوائق الخارجية و الضوضاء على النظام بغية الحصول على فعالية و كفاءة اعلى للنفق الهوائي اثناء اجراء التجارب بداخله .

يحتوي الجزء الاول من البحث على شرح موجز و مبسط عن الانفاق الهوائية (نفق الرياح) وطريقة عملها و اجزائها و انواعها، ثم سوف يتم دراسة مقارنة بين طريقتين مختلفتين في التحكم بالنفق الهوائي بحيث نقوم بتحليل النتائج و البيانات للوصول الى احسن التقنيات لتقليل الطاقة و رفع الكفاءة و الغاء تأثير التفاعل الداخلي للمتغيرات.

يشمل البحث على الرسومات البيانية و التخطيطية لتلك التقنيات مع المقارنة بينهم في مدى تأثرهم بالمتغيرات و سرعة الاستجابة و كفاءة النظام و مدى استهلاكه للطاقة.

ACKNOWLEDGEMENTS

I would like to express my sincere thanks to my supervisor Robert Whalley, for his great assistance and the patience shown throughout this research.

I would also like to thank Dr. Ala’a Abdul-Ameer, whose support and advice has been invaluable throughout this dissertation.

Finally, to all of my family – especially my Mother and my Brother - thanks for all your support and encouragement over the past few months.

Notations and Abbreviations:

$a_{i,j}(s)$	Element of A(s), $1<i,j>m$
$a_{i,j}, b_{i,j}, \ldots\ldots Y_{i,j}$	Coefficients of $Q(s)$
$A(s)$	Numerator of $G(s)$
$b(s)$	Polynomial
$b_0, b_1 \ldots\ldots b_{m-1}$	Coefficients of $b(s)$
$d(s)$	Denominator of $G(s)$
$f, f_1, f_2, \ldots\ldots f_m$	Output loop feedback gains
F	Outer loop feedback array
$G(s)$	Transfer Function array(Input/Output)
H	Feedback path gain
$h(s)$	Feedback path Function
$H(s)$	Feedback path compensator model
I_m	Identify matrix
J	Performance index
K	Forward path gain
$k(s)$	Forward path function
$k><h$	Outer product of k and h
$<k,h>$	Inner product of k and h
$K(s)$	Forward path pre-compensator model
L	Observer gain matrix

List of Figures and Tables:

Contents:

Chapter 1: Introduction

1.1 Research Background

From a control viewpoint, the factors in a process interrelate and create noticeable measurements. The noticeable factors are essential and regularly called outputs.

The process is likewise influenced by outside factors. These factors or variables that might be controlled by engineers are inputs of the process. Other outside factors are named turbulences (Y Zhu, 2001).

In applied control issues there commonly are various process variables which must be controlled and a number which can be operated, also product quality and throughput must usually be controlled. Each operated variable can influence the controlled variables which called process interactions.

Multivariable control methods fathom the issues of the multifaceted specification and demonstrating carefully, however the multifaceted nature of the fundamental arithmetic is much higher than introduced in conventional single-input, single-output control studies (P. Albertos Perez, 2013).

Multivariable Control Systems concentrates on control outline with constant reference to the applied features of operation. Tools of investigation and representation are constantly created as techniques for accomplishing a final control system design and evaluation (P. Albertos Perez, 2013). A simple physical example is shown in Figure (1.1).

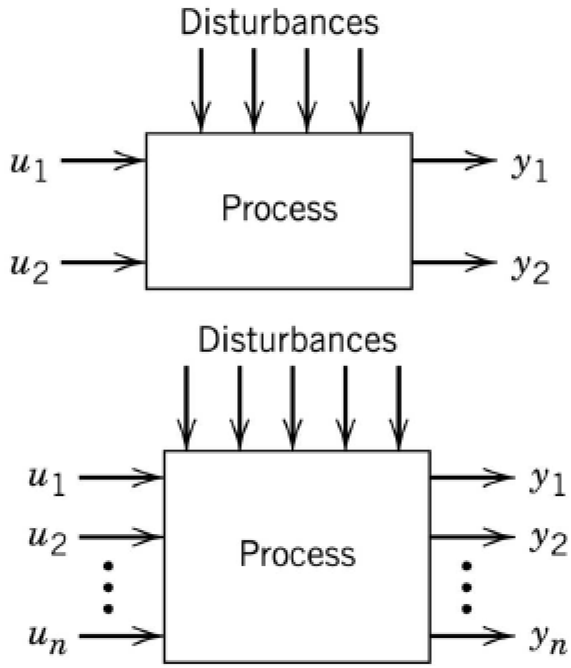

Figure 1.1: Multi-input, multi-output (MIMO) control system.
(Albertos.P and Sala.A, 2004)

Disturbances might be isolated in two sorts:

- Disturbances which might be straightforwardly calculated,
- Uncalculated disturbances which are just seen over their impact on the outputs.

A process is assumed to be dynamic when the present output gain depends on the present outer stimuli as well as on prior gains. Outputs of dynamic processes whose outer factors are not detected are regularly called time series (Ljung, 1987).

1.2 Research Problem Statement

The services of wind tunnel are available to the commercial aircraft industry, educational institutions, military and other government agencies requiring accurate air speed control and less turbulence to simulate actual flying conditions. To get the particular settings of operation, demanding control of the wind tunnel fan motor and vent actuators is wanted.

Controlled running cycles and high speed air in the wind tunnel working section may require large fan motor and high performance ventilation vanes which will increase the energy consumption leading to expensive charges to be added to Wind tunnel capital and maintenance costs.

The air velocity produced from either the fan motor or angle change in ventilation vanes should be researched with feedback regulators that can control the multivariable system and minimize the coupling between system outputs.

Also External disturbances may lead to incorrect measurements on the test subject. Therefore, Wind tunnel designers need to solve this issue by proper controller design in order to limit turbulence effects.

1.3 Research Aims and Objectives

Different approaches can be used to design the controller for a wind tunnel. The purpose of designing a controller for a wind tunnel will be shown using multivariable system techniques to provide the desired operational performance and minimization of the control effort required.
Two methods are discussed in this research. First the least effort approach (Whalley, R. and Ebrahimi, M., 1999) then the Nyquist Array approach (Rosenbrock, 1969).

Least effort approach attempts to advance the transient and steady state responses and accomplished closed loop stability with minimum response overshoot. The procedure includes two steps: analysis of inner loop then investigate outer loop design.
The above stated approach will be assessed against the Nyquist array method for gain comparison purposes. Additionally, Gershgorin's theorem will be used In order to apply single input single output control method, the system transfer function matrix has been compensated to become diagonally dominant.

Likewise the disturbance rejection properties of the system ought to be improved, Stability of the closed loop system should be accomplished with greatest conceivable decoupling among system outputs using methods such as the Relative gain array which helps to select the best approach.
Eventually, the energy consumed by the controllers will be computed and compared. The appraisal will include the difficulty of the controller and the general controller performance.

1.4 Dissertation Organization

This Dissertation is prepared in seven chapters as follows:

Chapter one contain the outline to this research. It includes the research background of multivariable control difficulties. The problematic statement as well as the objectives and goals are formulated.

Chapter two provides brief review of a wind tunnels, it shows the types of elements and history of wind tunnels and some technical information related to wind tunnel design.

Chapter three includes an introduction to multivariable systems and the control approaches that will be used to the wind tunnel model. A brief introduction of controllability tools and analysis method is also included.

Chapter four concerns the computation of the transfer function matrix for a wind tunnel model, the air flow dynamics in the wind tunnel and its open loop response.

Chapter five executes the least effort strategy and the whole approach to get the inner and outer loop controllers. The matlab Simulink and outcomes would be studied, containing the response, the disturbance recovery features and energy intemperance for the systems.

Chapter six includes an outline of the Nyquist array method for the wind tunnel model, Interactions and the analysis between system outputs will be discussed. The Gershgorin's band theorem and Diagonal Dominance will also be addressed.

Chapter seven includes a comparison with a discussed regardes the two control methodologies and the difficulties of applying each strategy.

Chapter eight contains the conclusions and the recommendations for future research work.

Chapter 2: Wind Tunnels Review

2.1 What is Wind Tunnel?

A wind tunnel is a tube or passage with rapid air going through it. Researchers and engineers put a model of a plane or a wing part in the passage, then study wind current over the model and how well the model will fly.

An example of wind tunnel shown in figure (2.1), Wind tunnels are also used for educational purposes and research projects enabling flight conditions to be simulated.

Wind passages and test models are costly to manufacture. That is the reason more associations are deactivating their wind passages and moving to PC modelling set up of physical models and passages.

In any case, physical passages are utilized to retest outcomes for PC modelling. Rechecking is crucial in numerous areas and thus wind passages are imperative.

Figure 2.1: Wind tunnel sample.

2.1.1 History of Wind Tunnel

Wind tunnels have been used for over 100 years. In fact, the Wright brothers used one to help them figure out how to build the world's first successful aircraft, the Wright Flyer.
The earliest enclosed wind tunnels were invented in 1871 and first designed by Frank Wenham; huge wind passageways were constructed through the 2nd World War. Wind tunnels were initially planned as a method for reviewing cars in free flight.
Currently, wind tunnels are used by NASA, Boeing, Northrop Grumman, and other organization that make aircraft and spacecraft.
Actually, NASA AMES, in Moffet Field, California, has the greatest wind tunnels at any one placed in the world, and moreover has the biggest wind tunnel on World, (Donald D. Baals and William R. Corliss, 1981).
As shown in figure (2.2) are old sample of a wind tunnel and NASA wind tunnel are shown.

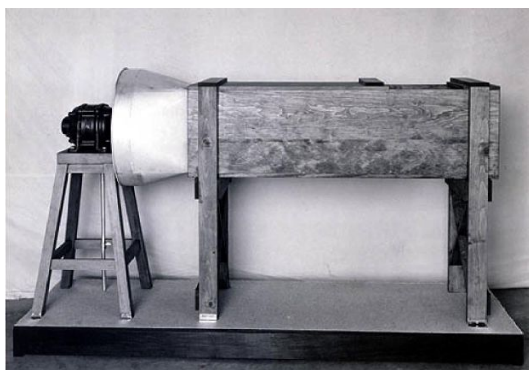

a) Old type of wind tunnel.

b) Modern wind tunnel with a plane model.

Figure 2.2: Old and modern wind tunnel model.

2.1.2 Air Flow in wind Tunnel

Normally air is exhausted through a tunnel utilizing a sequence of fans. Figure (2.3) shown the air flow on plane model, for massive wind tunnels, a sole substantial enthusiast is not useful, so a group of several fans could be utilized as a part of parallel to give adequate wind airflow.
Because of the total volume and air velocity development wanted, the fans might controlled by stationary turbofan motors as opposed to electric engines.
The wind current made by the fans is exceptionally nature turbulent because of the fan edge wave thus it is not specifically valuable for precise amounts.

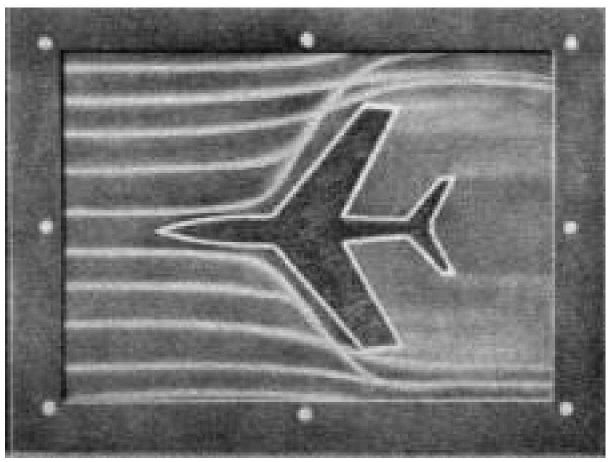

Figure 2.3: Air flow in wind tunnel.

In big wind tunnels because of the of viscosity impacts, the wind tunnel cross-section is regularly circle as opposed to square. Toward the sides of a tunnel of square type air movement might be nature turbulent. A closed loop tunnel delivers a better movement than a tunnel of square type.

2.1.3 Wind Tunnel Application

Wind tunnel is utilized as a resources of studying air flowing former solid substances in aerodynamic studies.

Wind-tunnel testing can also be useful to vehicles to decide approaches to decrease the influence needed to move the car on roadways.
Some automotive test wind tunnels have incorporated moving belts under the test vehicle in an effort to approximate actual condition.
In addition to vehicles, wind tunnels are used to study the airflow and wind loading around large structures such as bridges or office buildings.
Also wind tunnels are used for thermal evaluation of circuit boards, heat sinks, components and air velocity sensor calibration, (Wikipedia).

2.2 Elements of a Wind Tunnel

Generally, the wind tunnel is made up of different parts. They consist of a settling chamber, contraction cone, test section, diffuser and drive section as shown below.

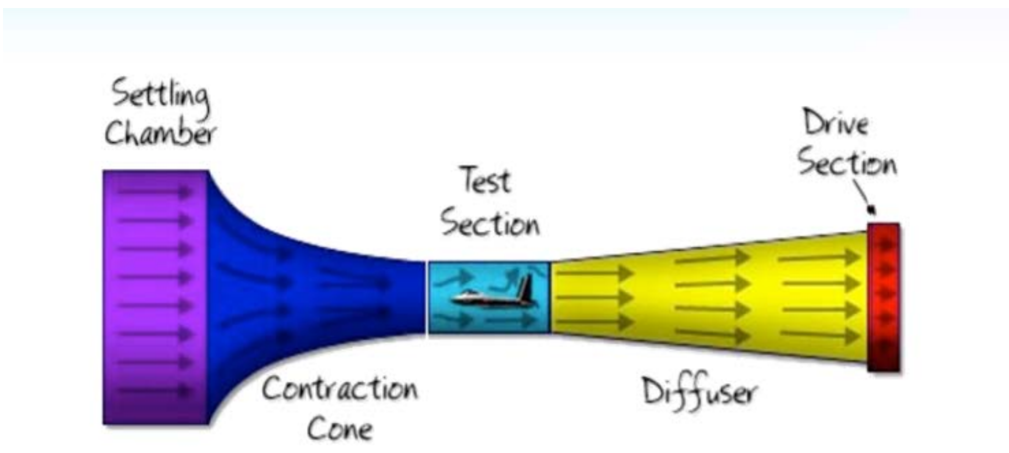

Figure 2.4: Wind tunnel components.

The air flows from the motivation section into the settling slot. The amount and the velocity of airflow might be managed by adjusting the velocity of the driver. After the settling slot, the air travels into the compression funnel where the velocity is expanded because of the state of the funnel, producing a pressure difference (Tabrej Khan, 2014).

The large fixed air velocity then arrives to working or check section then the model is studied. After that wind currents into the diffuser where the dissemination might be required.

Working with the principle above, the MARSWIT Mars Wind Tunnel located in The Planetary Aeolian Laboratory as shown below:

Figurer 2.5: MARSWIT Mars Wind Tunnel located in PAL.

2.3 Types of Wind Tunnels

Wind tunnels are intended for a particular reason and speed variety. There are a wide range of sorts of wind tunnels and a few distinctive approaches to arrange them.
Ordinarily, wind tunnels are categorized based on premise of air route. The air route might be either closed or open circuit.

For open circuit wind tunnel, the air sucked from outdoor environment and released back to out again. The air usually tracks a straight pathway from the access to the exodus of the wind tunnel.

In closed circuit, the air is distributed via the assistance of a power division. Occasionally a little measure of air of air is replaced by the outdoor to surge the quality and own roughly temperature regulator (V.L. Kakate, 2014).

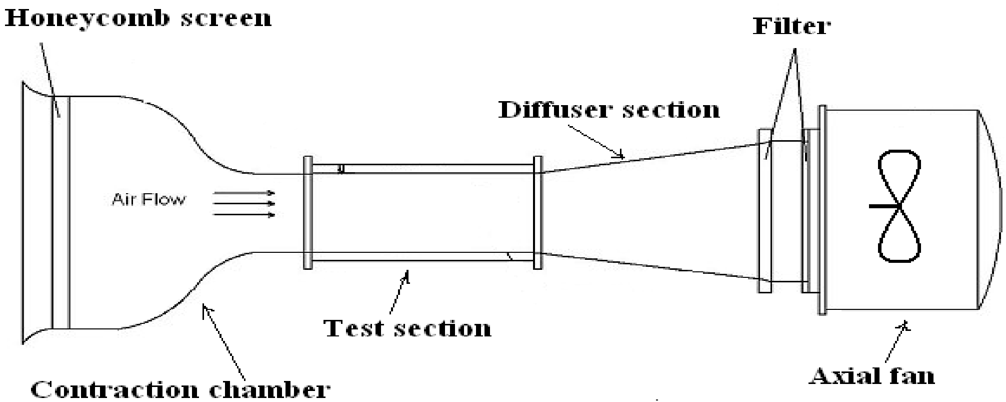

Figures 2.6: Open circuit wind tunnel.

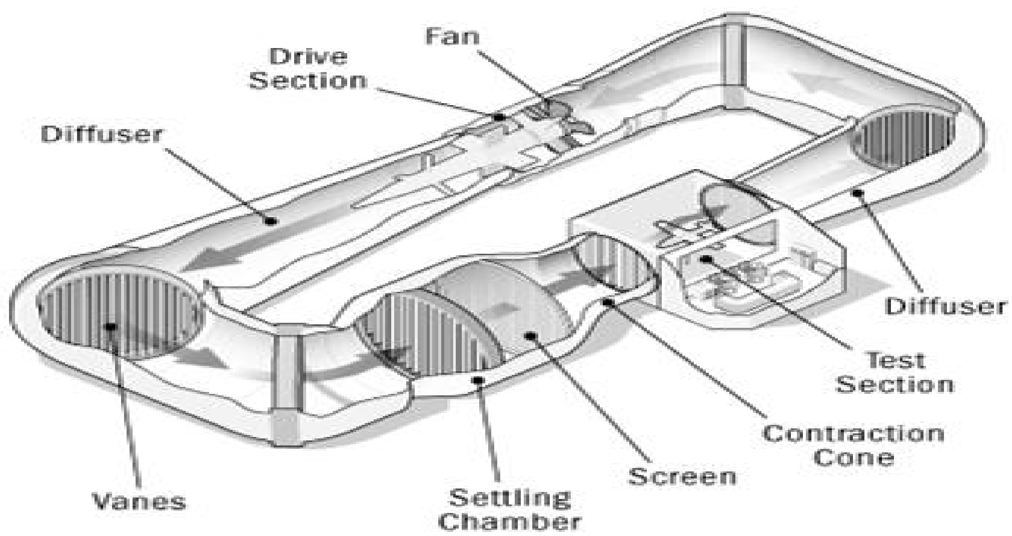

Figure 2.7: Closed circuit wind tunnel.

Wind tunnels with open and closed circuit got some main benefits and disadvantages, the comparison of these types are existing below.

Closed circuit wind tunnels	**Open circuit wind tunnels**
High construction costs.	Lower construction costs.
Purging after flow visualization using smoke and needing to mount a heat exchanger.	Being able to visualize the flow using smoke without needing to purge the tunnel.

high quality flow, independent of weather conditions and other activities in the building	Needing to mount extensive screens to obtain high quality flow.
Requires less energy.	Greater energy to run the wind tunnel.
Produces less noise.	High noise levels which may cause environmental problems.

Table 2.1: Comparing of closed and open wind tunnels.

Apart from this simple grouping, wind tunnels can be categorized based on:

A) Flow speed: Subsonic (M<0.8), Transonic (0.8<M<1.2), Supersonic (1.2<M<5.0) or Hypersonic (M>5.0).

B) Test type: Aeronautical, Automobile or Aeroacoustics

C) Construction elements: Metal structure, concrete style or complex structure wind tunnel.

D) Air pressure: atmospheric or variable- density.

E) Size: Ordinary or full-scale.

Subsonic
Open Return
Full Scale

Supersonic
Closed Return
Propulsion

Subsonic
Open Return
Smoke Tunnel

Figure 2.8: Examples of wind tunnel types from NASA Glenn Research Center

2.4 Electrical Concerns

Wind tunnel improvement includes mechanical and structural engineering. Though, few of the elements for example lighting plan, anemometer, exhaust fans and preparation of electrical supplies includes electrical and instrumentation engineering. The next paragraphs manage these features (V.L. Kakate, 2014),

A. Fans:
Exhaust fans could be built inside or outside of wind passageway. They moving air in trial cavity or push it from the trial cavity. Fans considered induction motor founded that might be triple or one phase sorts.

The quantity of fans needed is chosen via different variables, for example, the area of the wind tunnel for the speed variety of air, size of each fan and air volume transfer. The speed of fan, amount and type of fan edges used chooses the air volume transfer in wind tunnels.

B. Anemometer:
Anemometers are utilized to quantify the velocity of the air. Anemometer might be of next kinds:

1. Cup style – It is otherwise called rotational,
2. Propeller style - These same as the cup type, calculates the wind speed,
3. Ultrasonic anemometer - Ultrasonic, as its title recommends, includes sonic pulses to measure the wind velocity.

C .Lighting Plan

Classic wind tunnels have illuminations in it. Lamp fixtures are fixed into the internal partition of the tunnel. Accordingly, no disturbance to the air movement. LED arrangement are the greatest reasonable for the wind tunnels by way of they might be put alongside the tunnel partition with no influencing the air flow shape.

2.5 Measurements of Parameters

Speed and pressures of the air in wind tunnels are usually calculated thru numerous techniques. The velocity of air where inside the test section might be measured by Bernoulli's principle.

Airflow path nearby a test subject might be measured via tufts of yarn joined toward the aero-dynamic surfaces and the airflow wave drawing closer a surface might be imagined by rising threads in the airflow.

Fluid bubbles or smoke might be presented through the airflow source of the test element, and bubbles or smoke track might be snapped around the model.

The pressure distributions on the test model verifiably have been calculated by making several petty holes alongside the airflow route, and the multi-tube manometers used to determine holes pressure.

By using of pressure-sensitive coat also the Pressure distributions can be handily calculated, in which higher local pressure is specified by lowered fluorescence of the paint at that point.

In addition, pressure distributions on a test subject might be measured also by a wake survey accomplishment, where a solitary pitot tube is used to get multiple measurements downstream of the model, or a multiple-tube manometer can be mounted downstream.

Through digital sensors, every parameters measurements are procced to PCs.

Pressure distributions might be calculated thru the utilization of pressure -sensitive girdles, which pressure sensor with multiple ultra-miniaturized are combined to a flexible strip. The strip is involved by tape to the surface, and generate signals along its surface showing the pressure distribution (V.L. Kakate, 2014).

Chapter 3: Control Theory Review

3.1 Introduction to Control Systems

Control system main point is to drive a certain arrangement of process factors to act in imagined and recommended path by either satisfying a few necessities in the time/domain or accomplishing the greatest performances as stated in optimization index.

Engineers outline forms as indicated by the best of their insight in the field and by accepting few working situations. Afterward, the process will keep running under conditions that provide external disturbances which are typically not outstanding or found. Likewise, the features of the process will varying with time and load or even one of them. It is the part of the control system to adapt to these variations, giving thereby a proper conduct (P. Albertos and A. Sala, 2004).
The control duties scope differs broadly. The primary objective might be hold the process operating near the formal conditions. In further situations, change operating point of the plant from one to another or to follow a certain reference signal will be control goal.
In some situations, concern focused in gaining the supreme structures of the plant accomplishing, for example, the most extreme production, least vitality energy consumption, or least performance time for assumed task (P. Albertos and A. Sala, 2004).

All these diverse actions result in exceptionally particular control methodologies and strategies. Starting with logical and discrete-time controllers till advanced intelligent control systems where the artificial intelligence strategies give the framework, the multiple accessible appliances for control systems design are compatible in the integral control of a plant, few of them are used in a supportive technique (P. Albertos and A. Sala, 2004).

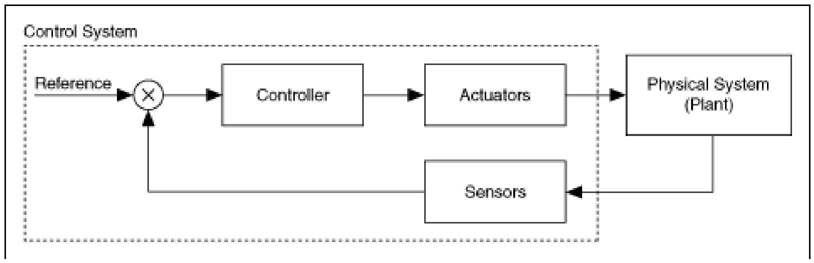

Figures 3.1: Combination of the control system and the plant.

3.1.1 The Control Design Problem

The finest control sub-system will simply give the greatest reasonable inputs to the process to satisfy the objectives. This has two primary outcomes:

1. If competences need aims which aren't erected into the process, the control may not succeed them.
2. The control system "select" the greatest input, between the likely ones, to achieve the objectives.

Depend on this confirmation there is a propensity these days to coordinate the process design and the control related to it. For example, in planning the control of a multiple-phase reactor process, the integral design of the control of the all system, in addition to driving the interaction between phases, can decrease the control effort and accomplish improved performances. Typically, a control system ought to be designed to work in cooperation with previously current process. The control design issue can be specified at native, supervisory or even plant-vest level (P. Albertos and A. Sala, 2004).

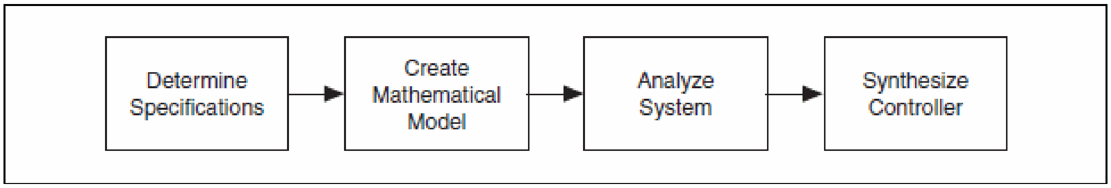

Figure 3.2: Typical steps involved in designing a controller.

3.1.2 Control Goals

In a general, some control aims can focused on are shown below:

- regulation,
- reference tracking,
- generation of sequential procedures,
- adaptation,
- error detection,
- supervision,
- coordination,
- Knowledge.

Some of these objectives might be conflicting so this is a multi-criteria choice issue. A reasonable exchange off is the most we can accomplish (P. Albertos and A. Sala, 2004).

3.2 Multivariable Systems

The majority of published work on feedback control systems concentrates on dynamic systems which are single-input, single-output (SISO). However, Multi-input, multi-output (MIMO) systems are termed to many systems found in the process, aerospace and marine industries have more than one input and output. Due to the effect of one input on more than one output, these systems pose a new set of problems when it comes to control. A traditional transfer function representation has been used as shown in Figure (3.3). Note that input $R_1(s)$ not only affects the output $Y_1(s)$ according to the transfer function $G_{11}(s)$, but also the output $Y_2(s)$by the cross-coupling term $G_{12}(s)$.

There is a similar effect for the output $Y_2(s)$ with respect to the inputs $R_1(s)$, $R_2(s)$ (N. Mort , 1997).

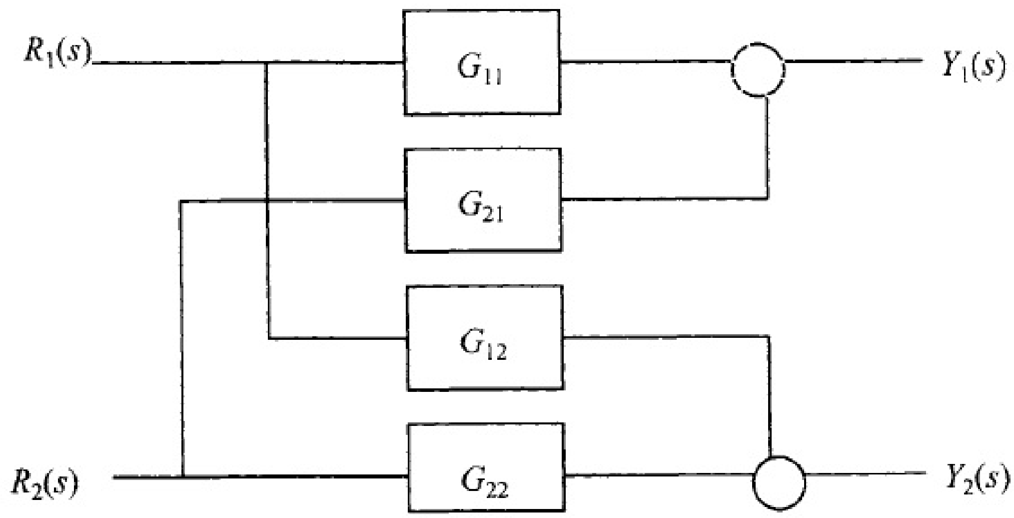

Figure 3.3: Block diagram of a two-input, two-output multivariable system.

MIMO processes are commonplace in industry. For example, in the rolling of strip steel, both speed and tension must be adjusted simultaneously in order to maintain the quality of the finished product. In the chemical process industry, the distillation column presents a good example of a non-linear, time-varying multivariable system. There are also numerous examples in the aerospace and marine industries such as military and civil aircraft, surface ships and submarines. In all these cases, there is more than one control surface/actuator and each actuator can influence a number of controlled variables. There is even a common example of a multivariable system in the home — the domestic electric shower unit. The effect of a cross-coupling term in the operation of a shower can be seen when a tap is opened elsewhere in the house while the shower is running. The flow is reduced and the temperature increases (often reaching unacceptably high levels!) In multivariable terms, we can consider the inputs to the shower as the pump voltage and the heating element voltage. The outputs are the flow rate and temperature of the water (N. Mort , 1997).

3.2.1 Multivariable Control

Many composite engineering systems can impact numerous actuators static and dynamic performance, because of arrangement behavior.
The type of programmed control is essential over the system in some situations, moreover values info about significant system variables that might be utilized for feedback control aims are deliver by some existing sensors.
Systems which contain multiple actuating control input and multiple sensor output might be considered multi variable systems (MIMO). The MIMO systems control goal is concurrently operating several input channels to acquire an attractive conduct of several output variables by (B. Veroemen, 1997).

3.2.2 History of Improvements in Multivariable Control

The initial researches on MIMO systems showed up in the 50th and accepted parts of non-interacting control. In the 60th, Rosenbrock (1970) work considered matrix methods to study objective and polynomial inquiries representation of multivariable systems.
The polynomial representation was additionally considered by Wolovich (1974). An extensive outline found in the books by Kailath (1980) and Vardulakis (1991).
Rosenbrock (1974) produced the utilization of Nyquist methods for multivariable control outline. The speculation of the Nyquist regulation and of root locus methods to the multivariable case can be found in the work of Postlethwaite and MacFarlane (1979).
The classical book by Wonham (1979) and in the book by Basile and Marro (1992) contained the geometric way to deal with multivariable state-space control design. An overview of classical design strategies for multivariable control systems can be found in (Korn and Wilfert 1982), (Lunze 1988) and in the two books by Tolle (1983), (1985).
Modern methods to frequency domain approaches can be found in (Raisch 1993), (Maciejowski 1989), and (Skogestad and Postlethwaite 1995).

Interface phenomena are argued in multivariable process control systems
about as far as a process control formulation in (McAvoy 1983). A modern, process-control situated way to deal with multivariable control is existing in (Morari and Zafiriou 1989). The numerical properties of few computational algorithms important to the range of multivariable control design are discussed in (Svaricek 1995).

3.3 Review of Multivariable Control Strategies

One of the main difficulties in designing controllers for multivariable systems is the presence of the cross-coupling terms. A substantial amount of effort has been expended in attempting to understand the effects of the interactions (A. Ichikawa & K. Furuta, 1994). A useful summary of these methods discussed below.

3.3.1 Non-interacting control (Decoupling control)

A standard method to MIMO control design comprises of the design of a pre compensator that conveys the system transfer matrix to diagonal type, with consequent design of the real feedback loops for the several single-input, single-output channels individually.
This permits the tuning of individual controllers in independent feedback loops, and it is thought to give an adequate control structure giving simplicity to process operators and maintenance workers review. The topic of non-interacting or decoupling control is depend on the works of Silverman (1970), Williams and Antsaklis (1986).

This design methodology is relatively simple to apply but it does impose severe constraints on the pre-compensator. Consider the simple block diagram structure shown in Figure (3.4) (P. Albertos, R. Strietzel and N. Mort, 1997).

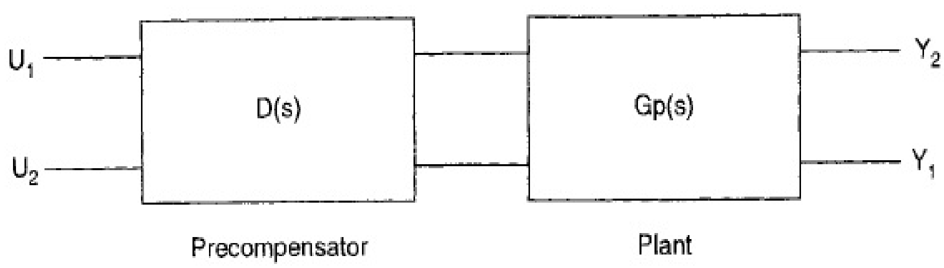

Figure 3.4: Pre-compensator and multivariable plant.

3.3.2 Nyquist-array methods

The stability of MIMO systems might be tested into a way like to the single input-single output type with applied of the Nyquist principle because of Rosenbrock (1974). Given confident settings are fulfilled. When the Nyquist array show diagonal dominance then it is critical condition. Extensively the cross-coupling implies in the system need to be adequately little to such an extent that altering the gain in single loop has just a restricted impact on the dynamics of the alternate loops (Dewi Jones, 1999).

Gershgorin's Theorem:
The Nyquist array plotted with Gershgorin's bands keeping in mind the end goal to check the system is column diagonally as per Gershgorin's bands theorem if not the merger of Gershgorin's bands encircle the plane's origin. Moreover, if the Gershgorin's bands not encircle the (-1, 0) point then the closed loop system stability is reached (Munro, 1972).
Figure (3.5) shows the Gershgorin band superimposed on the $\boldsymbol{g_{11}(s)}$ Nyquist plot from it is unmistakably the not covered critical point; the return variance is then diagonally dominant (Dewi Jones, 1999).

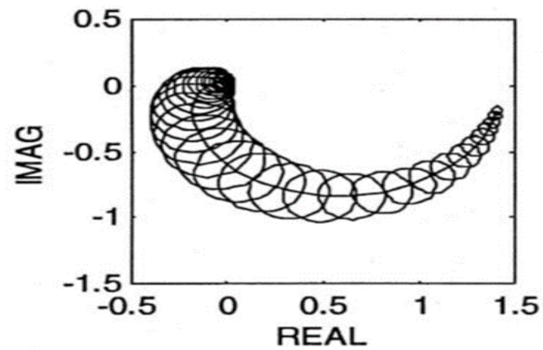

Figure 3.5: Direct Nyquist array

Stability of the Multivariable system:

It seems that this technique will produce slight extra info to the the system comparative stability with compensators. A technique by which the particular stability limits might be found but advises when diagonal dominance is not fulfilled- the shape of the stable region might be very complex Rosenbrock (1974).

A controller designing to minimize interaction:

Frequency domain design is regularly completed same work of the inverse Nyquist array on the other hand the direct Nyquist array (DNA) could be used for the causes specified by Maciejowski (1989).
The initial step in planning a controller is to lead the plant $G(s)$ with a pre-compensator$K_P(s)$, as in figure (3.6), in order to decrease interaction among the loops.

While immovably it's the return contrast which must be done diagonally dominant, the common repetition is to create the return ratio $G(s)K_P(s)$ diagonally dominant (Maciejowski, 1989). Obviously, $G(s)$ is not dominant since there is an assortment of frequencies where the Gershgorin band contains the origin.

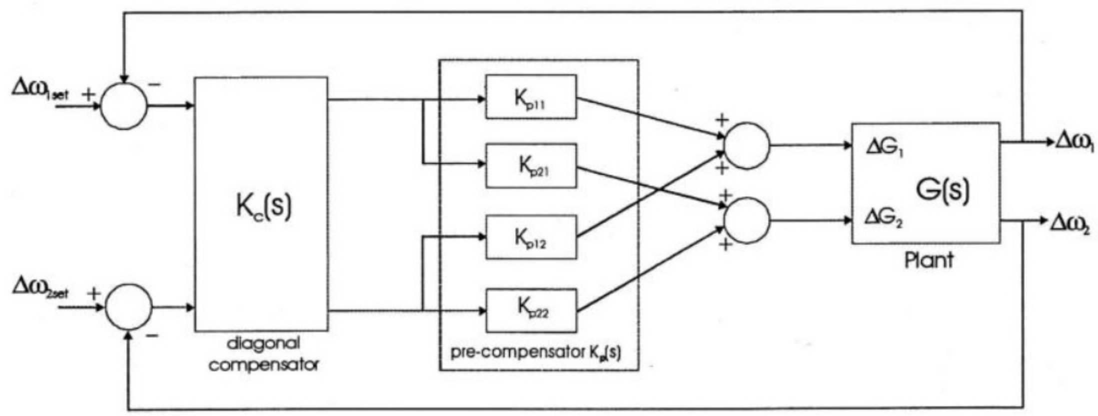

Figure 3.6: Block diagram for MIMO system with pre-compensator and diagonal compensator.

3.3.3 The Root Locus method

The root locus technique is a graphical method for sketching the locus of roots in the s-plane as a parameter is varied and has been utilized extensively in control engineering practice. Developed by Evans (1950) while he was a graduate student at UCLA, which the relative stability and the transient performance of a closed loop system are straight related to the position of the closed-loop roots of the characteristic equation in the s-plane.
It is frequently essential to amend one or more system factors in order to get proper root location and it is suitable to regulate the locus of roots in s-plane as a parameter varied since the roots is a function of the system's parameter.
Also it provides the engineer with a measure of the sensitivity of roots of the system a variation in parameter being considered (CAI Lilong, 2010).

3.3.4 Least Effort Methodology

The least effort technique was presented by (R Whalley, and M Ebrahimi, 1999. By analyzing Inner loop, to develop the dynamic performance output of the system. Afterward, the final design for outer loop is made to achieve robustness condition by suitable range of disturbance and acceptable steady state outputs decoupling.

3.3.5 PID Control

Ziegler-Nichols is a practical technique which help to configure (proportional-integral-derivative) controller's parameters. This method tends on analysis of stability where slightly stable gains are recognized. With empirical equations, the parameters for proportional, integral, and derivative components are introducesd by Zeigler and Nichols, 1942.

By identifying the gain and phase margins for the Gershgorin bands that will planned analytical formulas for the design of multi-loop PID controllers W.K. Ho et al. (1997). But this method is limited to a particular model structure. For MIMO systems the ultimate gain and frequency are defined based on Gershgorin bands and from the modified Ziegler-Nichols rules a design method is derived.

3.4 Controllability Analysis

Process "controllability" has been given different definitions, (Morari, 1983; Rosenbrock, 1970; Skogestad and Wolff, 1996; Ziegler and Nichols, 1943). Notwithstanding the different definitions, it is clear that controllability is an inherent property of the process, independent of the controller and demonstrates how simple it will be to control the process for both set-point tracking and disturbance rejection.
Controllability is interpreted as meaning the ability of the system to meet the requirement of set-point changes while resiliency is the ability of the system to recover from disturbances. Arkun and Downs (1990) did distribute a generalized methodology for launching input-output gains for processes with integrators. Though, the results of the controllability and resiliency measures (which are scale dependent) using the steady-state gain matrix developed by their method are varying with the physics governing separator operation.
Other scale independent measures, e.g. the relative gain array (RGA), gives realistic results though. Since the dynamic model is available, it is possible to evaluate "dynamic" controllability and resiliency measures,
(N. AL-Hatmi and M. Tham, 2006).

Relative Gain Array (RGA):

The RGA provides a quantitative criterion for selection of control loops that would lead to minimum interaction among the loops (Bristol, 1966). The RGA can be used to measure diagonal dominance, by the RGA-number. A small RGA number does not guarantee diagonal dominance. The relative gain array is expressed in the matrix form as:

$$\mathrm{RGA} = \begin{bmatrix} \lambda_{11} \lambda_{12} \\ \lambda_{21} \lambda_{22} \end{bmatrix}$$

3.1

The relative interaction array:

The relative interaction array (RIA) can be defined as the ratio of the absolute interaction and the interaction free transfer function as seen in the equation below (Zhu 1996).

$$\phi_{ij}(s) = \frac{\alpha_{ij}(s)}{g_{ij}(s)}$$

3.2

The Relative Interaction Array is similar to the RGA and is defined based on individual control loops and it can only measure interaction in individual loops. However, an overall interaction measure is defined along with the RIA which claims to lead to the best input-output pairing selection.

Condition number:

It is the ratio of the largest to smallest singular value in the singular value decomposition of a matrix (Belsley, David A.; Kuh, Edwin; Welsch, Roy E. 1980).

$$CN = \sqrt{\frac{\max \sigma}{\min \sigma}} \qquad \textbf{3.3}$$

Where the singular values are the positive square roots of the eigenvalues of:

$$K^T K \,(r = \text{rank of } K^T K) \qquad \textbf{3.4}$$

The system is sensitive to uncertainty and shows problems in controlling (ill-condition) when large condition number is shown.

Niederlinski Index:

NI uses only steady state gains of the transfer function matrix (Niederlinski, 1971).

$$N = \left[\frac{|G|}{\prod_{i=1}^{n} g_{ii}}\right] \quad \textbf{3.5}$$

The method is used to avoid pairing of variables which would be unsatisfactory, it also allows us to test the stability in some cases.
If a negative value for the NI, when all the control loops are closed, implies the system will be integrally unstable for all possible values of controller parameters.
And if NI = 1 indicate at least one the off diagonal terms are zero which mean the system can be diagonal dominate.

Chapter 4: Wind Tunnel Modeling

The structure of a representative wind tunnel is shown in Figure (4.1) where the major components are labelled. As showed, the two inputs are fan speed $\mathrm{w}(t)$ and the ventilation vane angle $x(t)$, the outputs which are to be controlled are the air velocity at the working section $v_1(t)$ and at the fan exit $v_2(t)$.

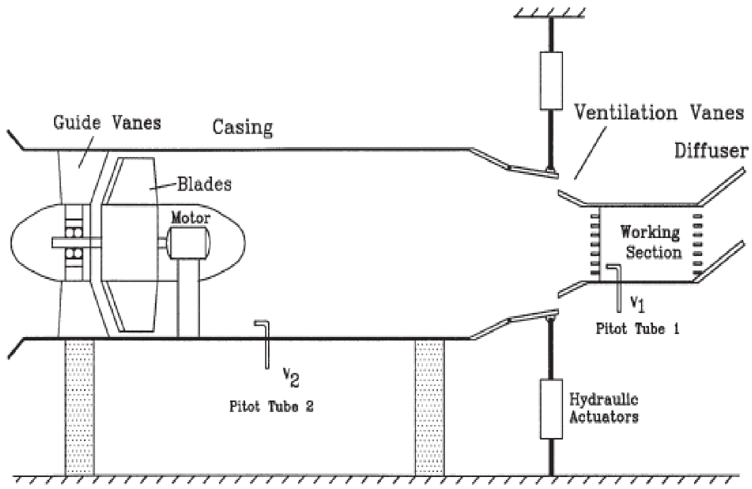

Figure 4.1: Wind Tunnel Arrangement

An analysis of this configuration is existing by Whalley.R and Mitchell.D (1997) where the impedance, matrix quadratic model for the system was derived.

The velocity of the air stream in the working section can be attuned by varying the fan motor speed or by changing the ventilation vane angles, which are hydraulically actuated.
The cross-sectional area of the working section, where the aerodynamic testing is conducted, is less than a quarter of that of the casing. This enables 'high' air speeds to be generated in the working section. Pitot tubes are used to calculate the air velocity at locations shown (Whalley.R and Mitchell.D, 1997).

4.1 Mathematical Model and Transfer Function

In command to determine the related transfer functions the ventilator opening are first set at their middle range values then flow measurements of velocities v_1 and v_2 are taken for stochastic or deterministic variations in the fan motor speed ,thus allowing the creation of column one of transfer matrix .

Comparable column two of the transfer matrix, relating the velocities v_1 and v_2 to the ventilation vane setting, can be achieved by running fan motor at its mean speed and then modifying the ventilation vane sittings. Quantities of air speed, v_1 and v_2 were recorded again previous to starting, by any of the practices obtainable, column two of transfer function matrix (Whalley.R and Mitchell.D, 1997).

For percentage changes in the input and out outputs probable transfer matrix is, in time scaled form,

$$\begin{bmatrix} v_1(s) \\ v_2(s) \end{bmatrix} = \begin{bmatrix} \frac{e^{-1.5t}}{s^2+4.0s+8.0} & \frac{0.5e^{-0.3t}(s-4.0)}{(s+4.0)(s^2+4.0s+8.0)} \\ \frac{2.0e^{-1.5t}}{(s+8.0)(s^2+4.0s+8.0)} & \frac{e^{-0.3t}(s+1.0)}{(s+8.0)(s^2+4.0s+8.0)} \end{bmatrix} \times \begin{bmatrix} \overline{\omega_f}(s) \\ \overline{\chi}(s) \end{bmatrix} \quad \mathbf{4.1}$$

In equation 4.1 the coefficients allocated were the best rounded approximate that could be gotten from the noisy measurements and the finite time lags were mostly because of the actuator delays. Accordingly,

if

$$[\omega_f(s), \chi(s)]^t = [e^{-1.5t}\,\overline{\omega_f}(s), e^{-0.3t}\,\overline{\chi}(s)]^t$$

Then the rational transfer function matrix is

$$y(s) = G(s)u(s)$$
4.2

where

$$G(s) = \begin{bmatrix} \frac{1}{(s^2+4s+8)} & \frac{0.5(s-4)}{(s+4)(s^2+4s+8)} \\ \frac{2}{(s+8)(s^2+4s+8)} & \frac{(s+1)}{(s+8)(s^2+4s+8)} \end{bmatrix}$$

$$y(s) = [v_1(s), v_2(s)]^t$$

and

$$u(s) = \left[w_f(s), x(s)\right]^t$$

4.2 Open Loop System Response

The time –scaled, time – domain response of the system to a 1 per cent change in motor speed and then to a 1 per cent change in ventilation vane angle, respectively, are shown in figures 4.1 and 4.2. In Figure 4.1 the percentage change in the velocities $v_1(t)$ and $v_2(t)$ both exhibit oscillatory increase to their steady state conditions, owing to reflected pressure waves from the tunnel boundaries, following changes in the fan speed.

Increasing the ventilator vane angle by 1 per cent causes a sudden drop in pressure and hence a surge in air flow along the tunnel. For a short period of time this flow increase causes, as shown in figure 4.2, an rise in velocity in the working section of the tunnel, which rapidly diminishes as new steady state velocity, which is lower than earlier, is recognized as shown by $v_1(t)$.

The air velocity change, $v_2(t)$, at the fan exit rises, however, due to lower back-pressure encountered, and settles to greater steady state value following oscillatory transient (Whalley.R and Mitchell.D, 1997).

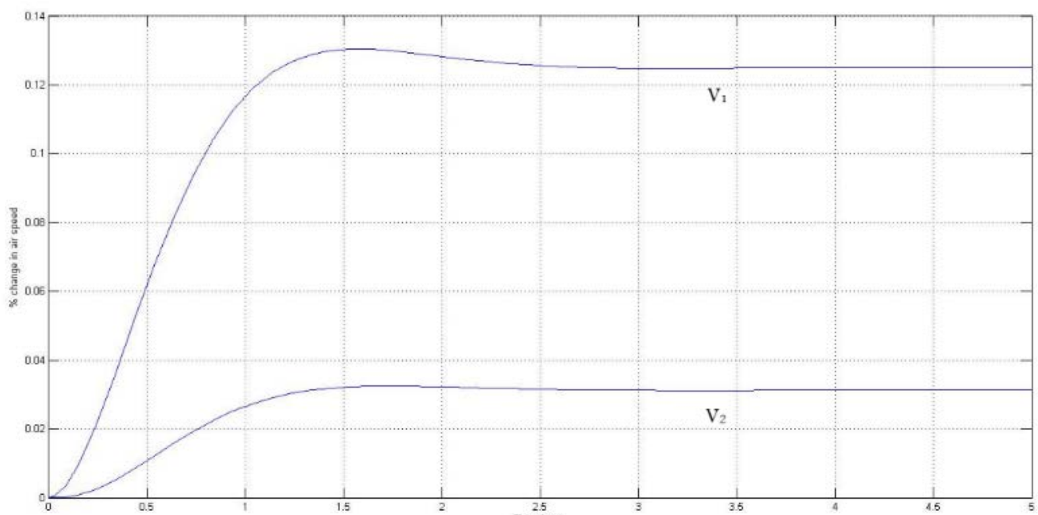

Figure 4.2: Change in air velocity following 1 per cent change in fan motor speed.

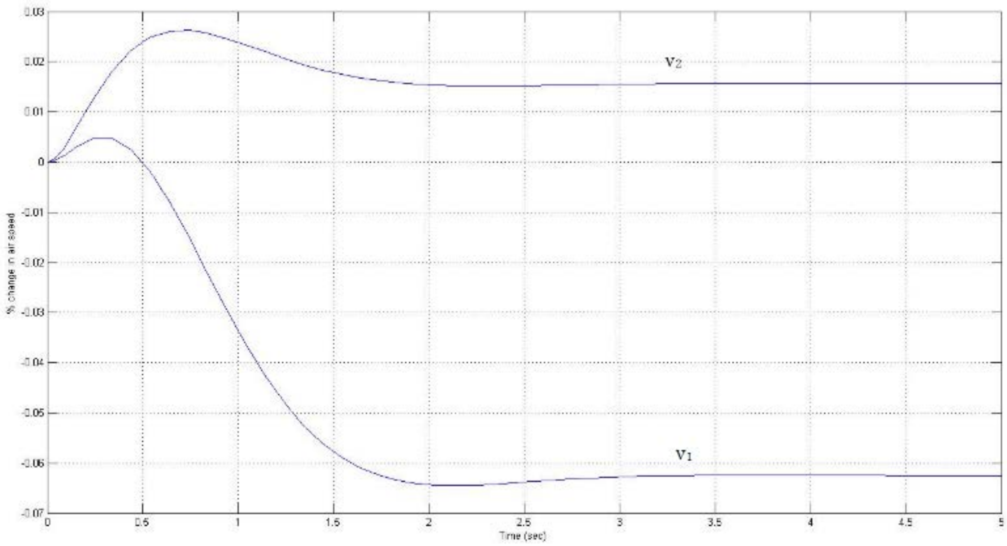

Figure 4.3: Change in air velocity following 1 per cent change in ventilation vane angle.

4.3 Performance Specification

To begin the design of a suitable compensator for the wind tunnel, it was necessary to have a specification detailing the performance requirements for the compensated system.

The proposed specification is outlined below in Table 4.1

System Parameter	Required Tolerance
Steady state error:	no steady state error ($e_{ss=0}$)
Overshoot:	Maximum 10%

Settling time:	Less than 6 %
Rise time:	Less than 3 seconds
Interaction:	maximum 20%
Energy dissipation:	Least energy control

Table 4.1: Performance specification

Chapter 5: Least Effort Controller

The following mathematical derivation is based on Whalley and Ebrahimi (2006), Appendix (C) contains the manuscript which explain a control approach for using an inner-loop and an outer-loop feedback structure.

In the wind tunnel design process, a dual loop will be applied. The inner loop and the outer loop are employed to achieve required steady state and satisfactory disturbance recovery.

5.1 Inner-loop Design

According to equation (4.2), the open loop transfer function matrix for Wind Tunnel (neglecting finite time delays) is:

$$G(s) = \begin{bmatrix} \frac{1}{(s^2+4s+8)} & \frac{0.5(s-4)}{(s+4)(s^2+4s+8)} \\ \frac{2}{(s+8)(s^2+4s+8)} & \frac{(s+1)}{(s+8)(s^2+4s+8)} \end{bmatrix} \qquad \textbf{5.1}$$

This system model can be arranged as:

$$G(s) = L(s)\ \frac{A(s)}{d(s)}\ R(s)\ \Gamma(s)$$

So the transfer function matrix in equation (5.1) could be written as:

$$G(s) = \begin{bmatrix} \frac{s+8}{s+4} & 0 \\ 0 & 1 \end{bmatrix} \frac{\begin{bmatrix} s+4 & 0.5(s-4) \\ 2 & s+1 \end{bmatrix}}{(s+8)(s^2+4s+8)} \qquad \textbf{5.2}$$

where

$$L(s) = \begin{bmatrix} \frac{s+8}{s+4} & 0 \\ 0 & 1 \end{bmatrix}, A(s) = \begin{bmatrix} s+4 & 0.5(s-4) \\ 2 & s+1 \end{bmatrix}$$

and

$$d(s) = (s+8)(s^2+4s+8)\ , \qquad R(s) = \mathit{\Gamma}(s) = I$$

hence

$$< h\ A(s)k\ >= [h_1 \quad h_2] \begin{bmatrix} s+4 & 0.5s-2 \\ 2 & s+1 \end{bmatrix} [k_1\ k_2] \tag{5.3}$$

Which can be re-written in the following format:

$$< h\ A(s)k\ >= [1 \quad s] \begin{bmatrix} 4 & -2 & 2 & 1 \\ 1 & 0.5 & 0 & 1 \end{bmatrix} \begin{bmatrix} k1\ h1 \\ k2\ h1 \\ k1\ h2 \\ k2\ h2 \end{bmatrix} \tag{5.4}$$

Parameters k and h should be calculated, the gain ratio n substituted to formulate the matrix Q.

Let $k2 = nk1$, then substituting for $k2$ yields:

$$Q = \begin{bmatrix} 4-2n & 2+n \\ 1+0.5n & n \end{bmatrix} \tag{5.5}$$

5.2 Determining of Controller Zero

In Order to design the inner loop that takes the form:

$$< h\ \frac{A(s)}{d(s)}k\ >= \frac{b(s)}{d(s)} \tag{5.6}$$

Root locus approaches will be used according to equation (5.6) and the equation for the Root Locus is:

$$\frac{b(s)}{d(s)} = -1$$

where

$$b(s) = b_o(s + x)$$

The roots of denominator $d(s)$ and the numerator $b(s)$ should be calculated to design the inner loop for the system and it can be noted that the poles of the system lie at (-8), (2+2j) and (-2-2j). So to attract poles further to the left of imaginary axis which mean faster response, A zero $(x + 2)$ is chosen.

The root locus diagram is initially plotted with $b_o = 1$ and $x = 2$ as shown in figure (5.1).

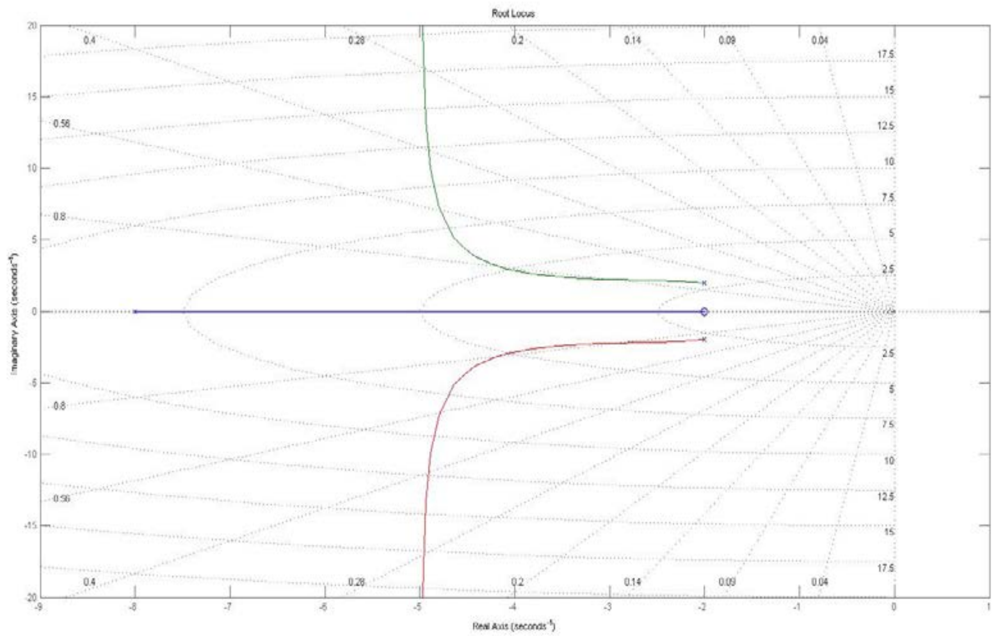

Figure 5.1: The Root Locus diagram

From the above root locus diagram, to achieve an acceptable overshoot and reducing the settling time for the system, $b_o$at 16 is chosen as shown in figure (5.2).

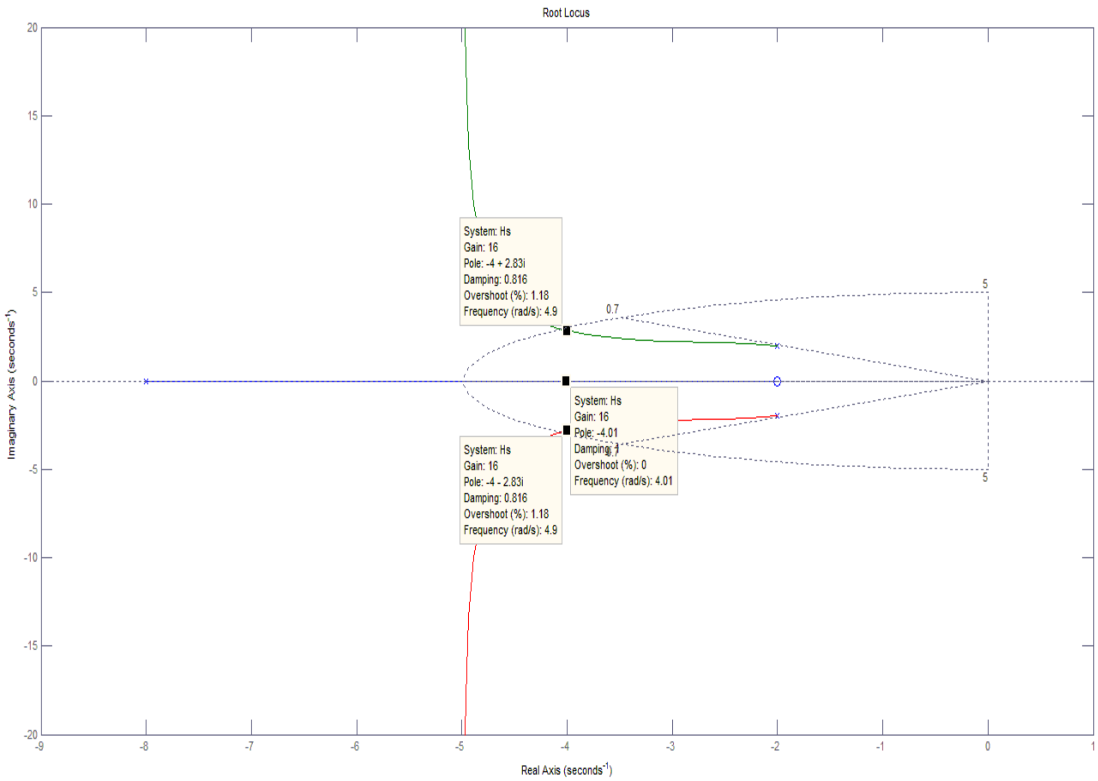

Figure 5.2: b_o= 16 in the Root Locus diagram.

It can be noted when the unity feedback closed loop system, the new poles are present in figure (5.3) and step response become more efficiently and keeping acceptable dynamics as shown in figure (5.4).

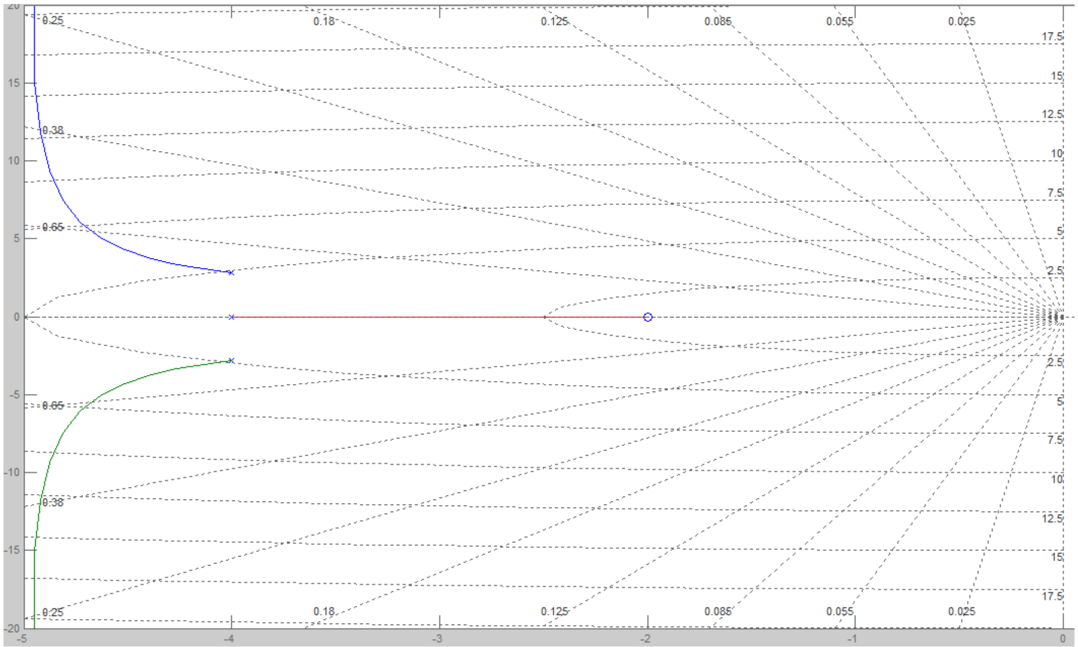

Figure 5.3: Poles at closed loop with unity feedback.

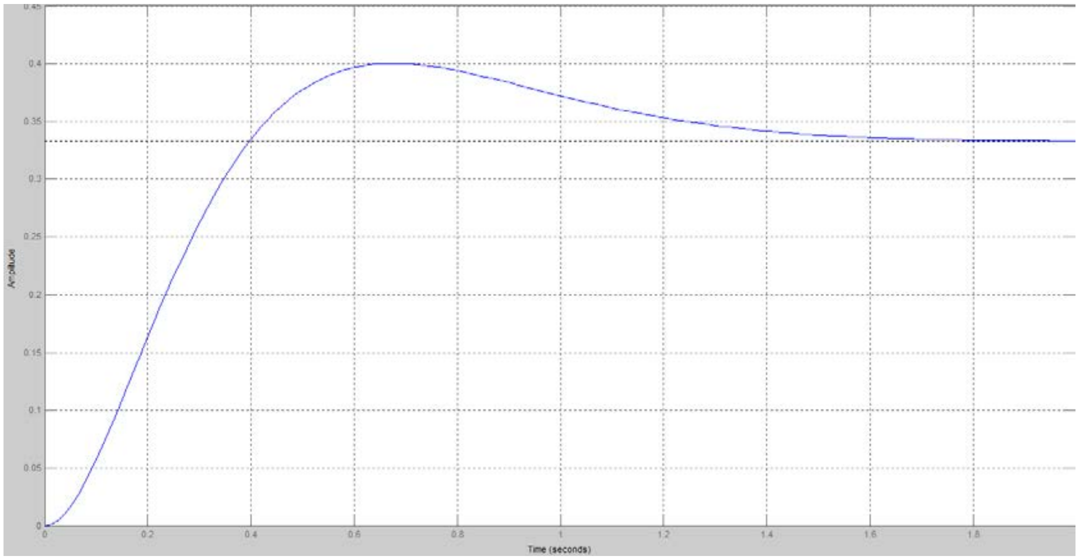

Figure 5.4: Closed loop with unity feedback step response.

hence

$$b(s) = 16\begin{bmatrix}2\\1\end{bmatrix} \qquad \textbf{5.6}$$

5.3 Wind Tunnel Optimization

It can be calculate the specific gain ratio n from the performance index J which is:

$$J = (1 + n^2) b^T \, (Q^{-1})^T \, Q^{-1} \, b$$

Substituting for b and Q in the performance index equation yields:

$$J = \frac{2048.\,(1. + n^2)\,(-8.\,n + 5.\,n^2 + 4.)}{(-4.\,n + 5.\,n^2 + 4.)^2} \qquad \textbf{5.7}$$

The performance index against gain ratio shown in figure (5.5).

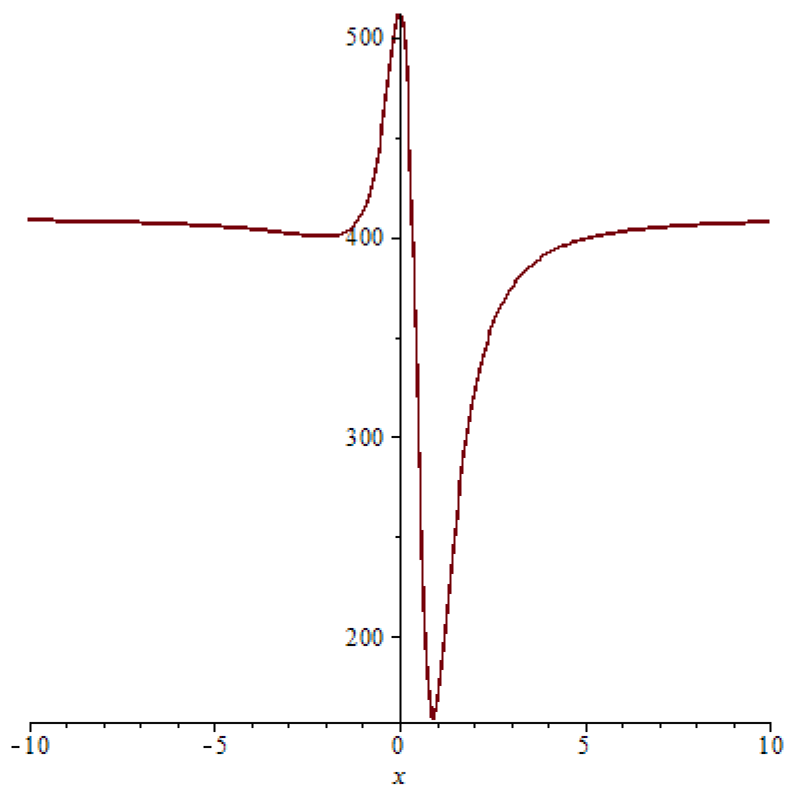

Figure 5.5: The performance index versus gain ratio.

To get the minimum value of J, the value of n should be measured by the function differentiation with respect to gain ratio and equating to zero.

hence

$$\frac{\partial J}{\partial n} = \frac{4096.n\,(11.n^2 + 12.n - 20.)}{(-4.n + 5.n^2 + 4.)^3} = 0 \qquad 5.8$$

and roots are:

$$[\,[n = 0.],\ [n = 0.9090909091],\ [n = -2.]\,]$$

From the graph of performance index against gain ratio it can be noted that J minimum and it exists at $n = 0.9090$ as shown in figure (5.6).

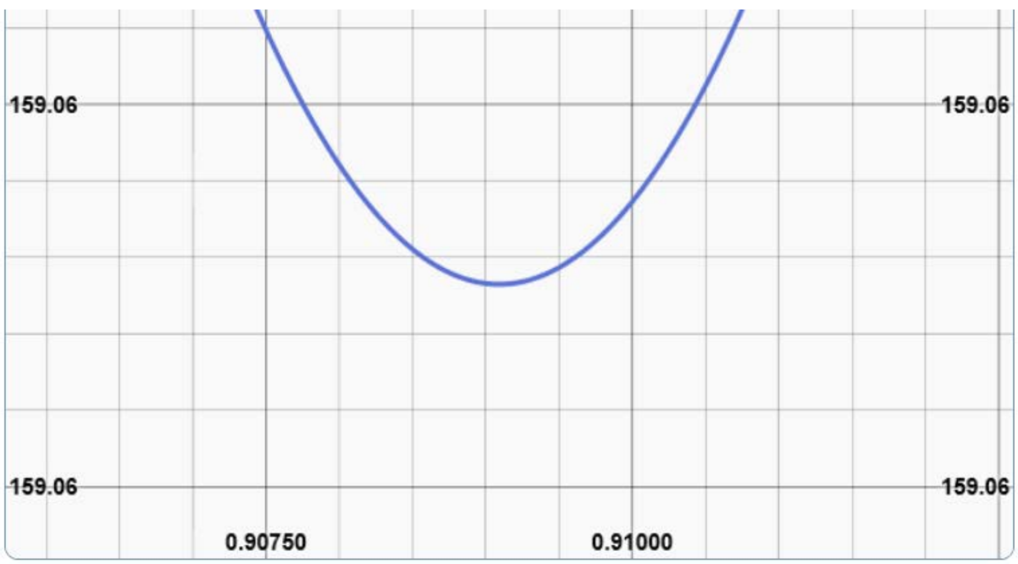

Figure 5.6: The performance index versus gain ratio.

Now the feedback measurement gains could be calculated with , b:

$$h = \frac{Q^{-1}}{K_1}\, b$$

hence

$$h = \left(\frac{s+4}{s+8}\, h_1\,, h_2\right) = \left(\frac{s+4}{s+8}\, [7.766], 5.175\right) \qquad 5.9$$

and by substituting for n in Q and assuming K_1 = 1, results in

$$K = \begin{bmatrix} 1 \\ 0.9090 \end{bmatrix} \qquad \textbf{5.10}$$

From previous information, the closed-loop system configuration block diagram when the minimum-control-effort regulator, given by equation (5.6) is shown in Figure 5.7).

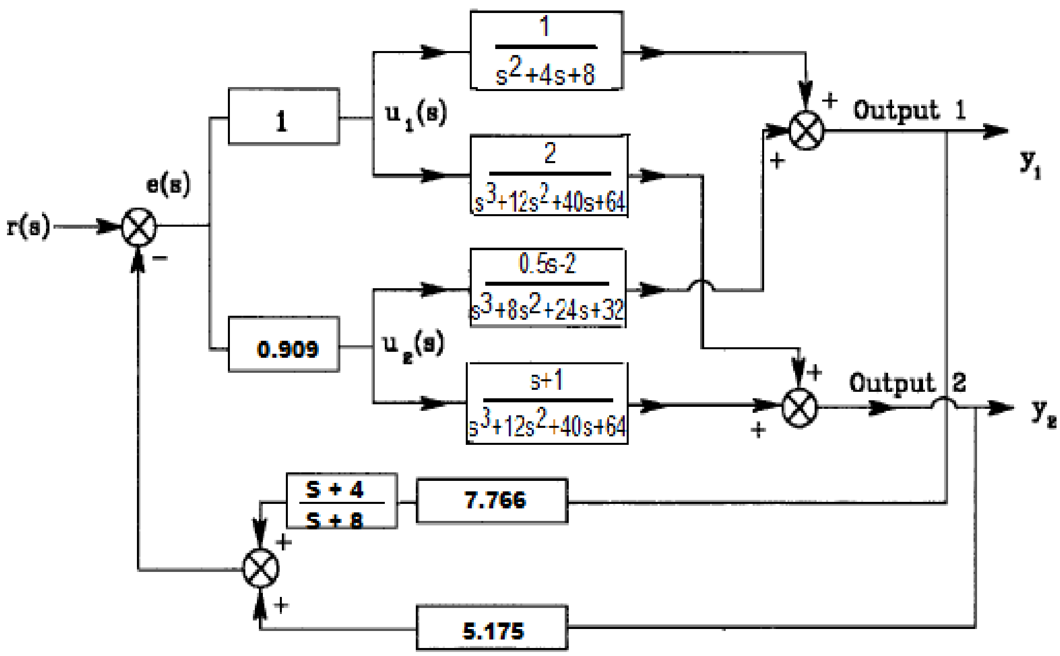

Figure 5.7: Closed-loop system (Inner loop) block diagram.

For a step input, the air velocity in the working section v_1& $v_2$responses are shown in figure (5.8).

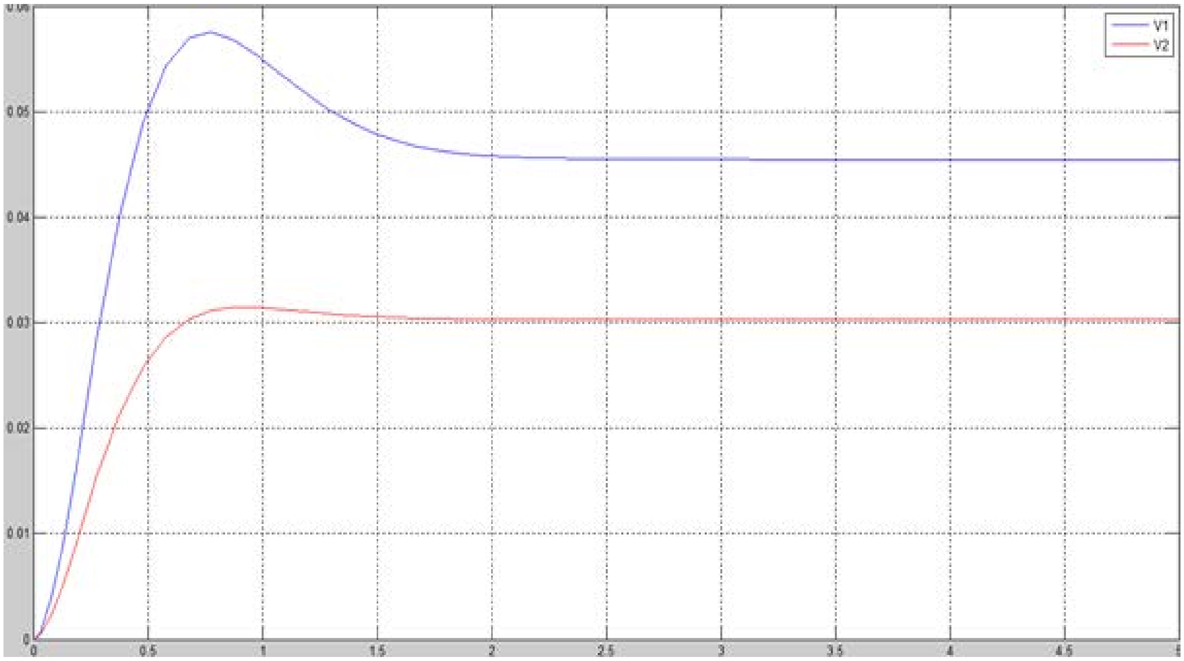

Figure 5.8: Closed-loop output responses $y_1(t)$ and $y_2(t)$ following a step input of unity.

Also Following a unit step with $R = 22$, fixed to provide uniformity among input set point and steady state output variations at v_1, the responses shown in figure (5.9).

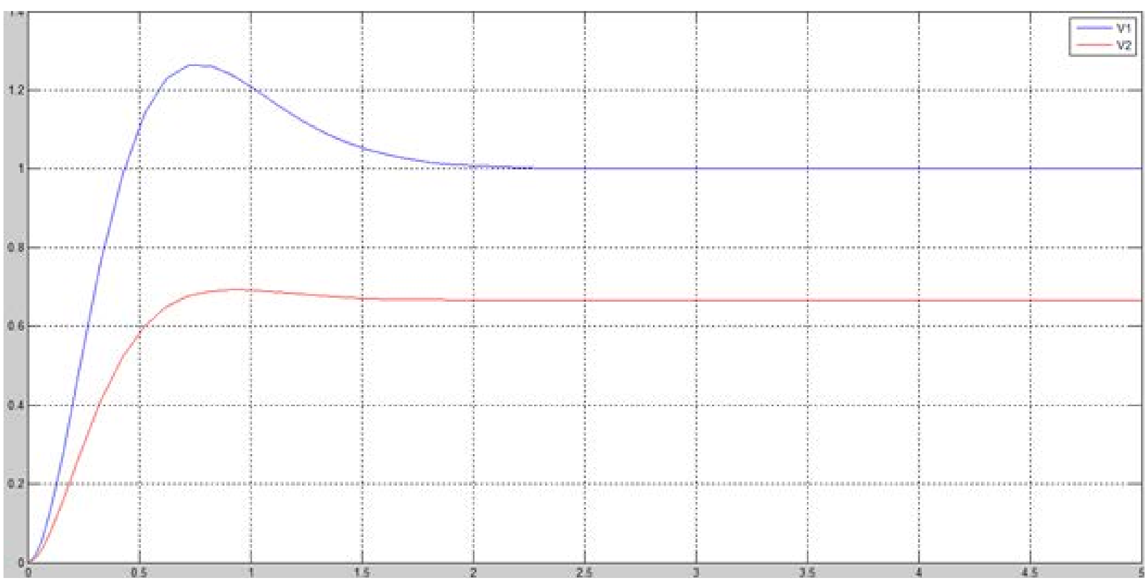

Figure 5.9: Closed-loop output responses $y_1(t)$ and $y_2(t)$ following a step input of unity.

It can be noted from figures above that the output responses are faster than the open-loop system output responses which produce slow reaction as shown in pervious chapter.

Hence, internal loop schemes shows suitable dynamics in terms of settling time and rise time.

5.4 Outer Loop design

To design the outer loop controller consuming equation given by:

$$P = \left(G(0)^{-1} + K(0) >< h(0)\right)S_s \ . \ (I - F.S_s)^{-1}$$
5.11

All matrices involved should be calculated at steady state, by substituting $S = 0$ in the open loop transfer function matrix, the feed forward and feedback gains yields:

$$G(0) = \begin{bmatrix} \frac{1}{8} & -\frac{2}{32} \\ \frac{2}{64} & \frac{1}{64} \end{bmatrix} \quad \mathbf{5.12}$$

hence:

$$G(0)^{-1} = \begin{bmatrix} 4 & 16 \\ -8 & 32 \end{bmatrix} \quad \mathbf{5.13}$$

and

$$K(0) = \begin{bmatrix} 1 \\ 0.9090 \end{bmatrix} \quad \mathbf{5.14}$$

$h(0) = \begin{bmatrix} 3.883 & 5.1750 \end{bmatrix}$ **5.15**

hence:

$$K(0) \times h(0) = \quad = \begin{bmatrix} 3.883 & 5.175 \\ 3.529 & 4.704 \end{bmatrix}$$

Since the closed loop steady state interaction of the system between outputs could be limited to 20% the value is assumed as:

$$= \begin{bmatrix} 1 & 0.2 \\ 0.1 & 1 \end{bmatrix} \qquad \textbf{5.16}$$

Now the feedback gains f should be selected at different values from 0.1 to 0.9 to investigate the effect on the response of closed loop in order to design the valuable control system approach.

Inserting $G(0), S$s, $K(0)$ and $h(0)$ values and with different F values into equation (5.11) results in:

For $f = 0.1$, then $F = \begin{bmatrix} 0.1 & 0 \\ 0 & 0.1 \end{bmatrix}$

hence:

$$P = \begin{bmatrix} 11.3953 & 25.5327 \\ -0.4475 & 39.7787 \end{bmatrix}$$

As far as conventional forward and feedback path recompenses could be calculated by substitution values in equation:

$$H = P^{-1}K(s) >< h(s) + F \qquad \textbf{5.17}$$

hence:

$$H = \begin{bmatrix} 0.2384 & 0.1845 \\ 0.0902 & 0.2203 \end{bmatrix}$$

by repeating calculation,

at $f = 0.5$, then $P = \begin{bmatrix} 25.0523 & 50.5136 \\ 5.6742 & 72.7544 \end{bmatrix}$

and $H = \begin{bmatrix} 0.6384 & 0.1845 \\ 0.0902 & 0.6203 \end{bmatrix}$

at $f = 0.8$, then $P = \begin{bmatrix} 140.4495 & 226.1176 \\ 99.4361 & 258.5979 \end{bmatrix}$

and $H = \begin{bmatrix} 0.9384 & 0.1845 \\ 0.0902 & 0.9203 \end{bmatrix}$.

The inner and outer loop controller block diagram of the system is shown in figure (5.10) and representation of conventional structure shown in figure (5.11).

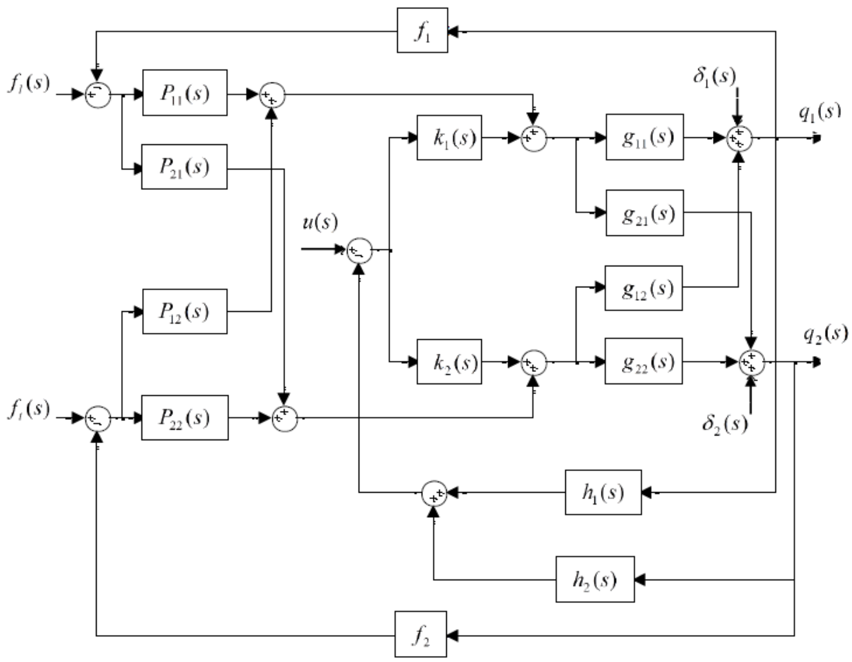

Figure 5.10: Inner and outer closed loop controllers block diagram.

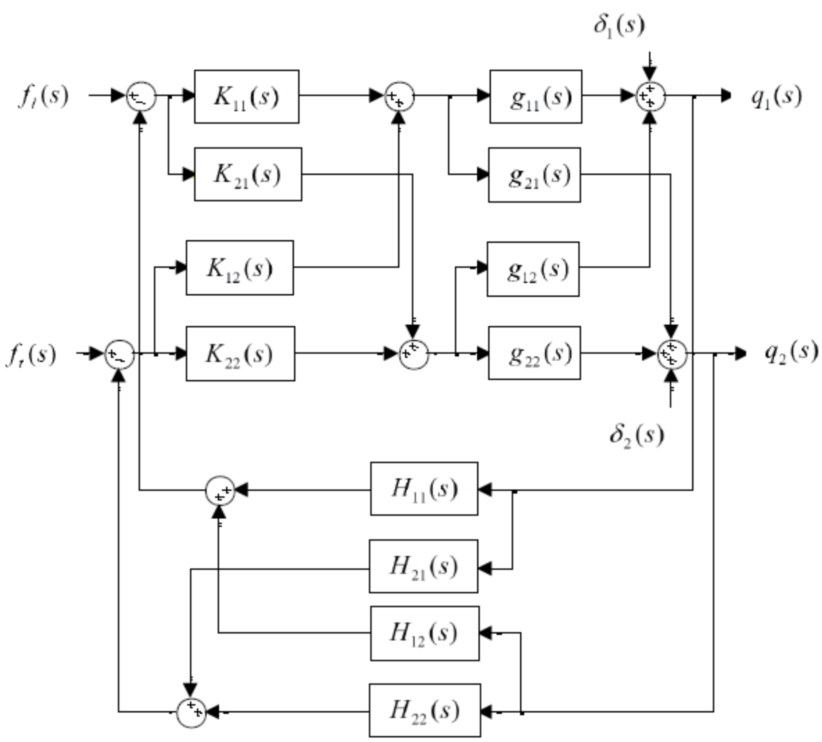

Figure 5.11: Conventional multivariable feedback structure block diagram.

From the block representation simulation, closed loop velocities v_1 and v_2 output responses for 1 per cent step input on motor speed at different f values shown in figure (5.12):

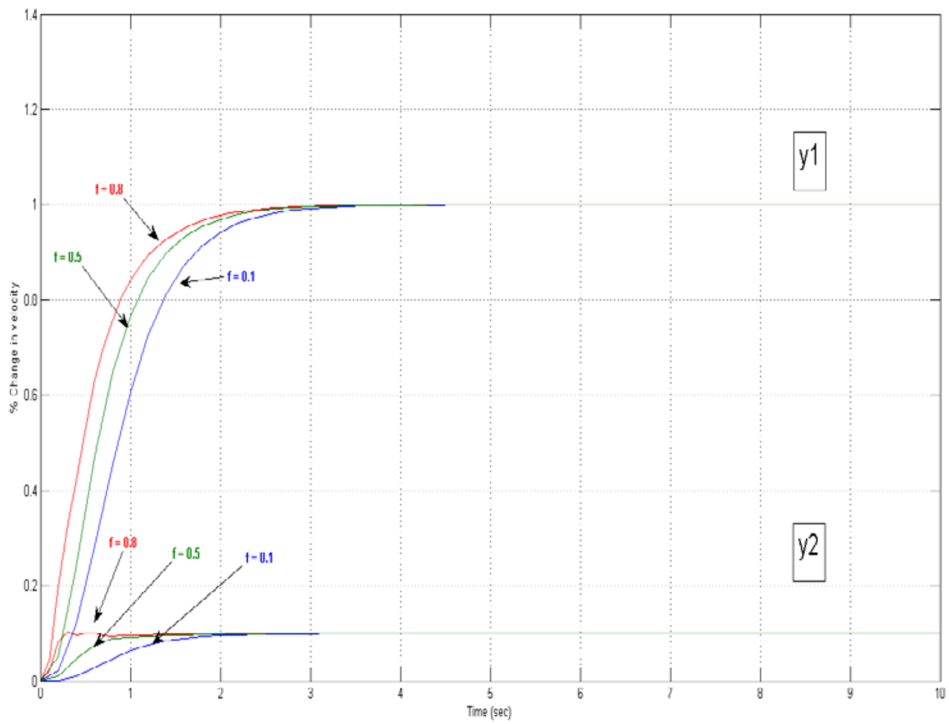

Figure 5.12: Output responses $y_1(t)$ and $y_2(t)$ following a step input of unity on motor speed at f =0.1, 0.5 and 0.8.

It shown from figure (5.12), the closed loop output responses is over damped and with no oscillatory behavior.

Velocity response in the working section $y_1(t)$ reaching steady state in almost 3 seconds with zero steady state errors, also with higher f (i.e. = 0.8) response speed will increase and that means a fast rise time.

The velocity in casing section $y_2(t)$ reaching steady state in fewer than 2 seconds with non-steady state error, it can be noted that an increase in the speed of the response and decrease in the settling time when f value go higher (i.e. = 0.8).

The closed loop velocities $v_1\ and\ v_2$ output responses for 1 per cent step input on ventilation vane angle at different f values is shown in figure (5.13):

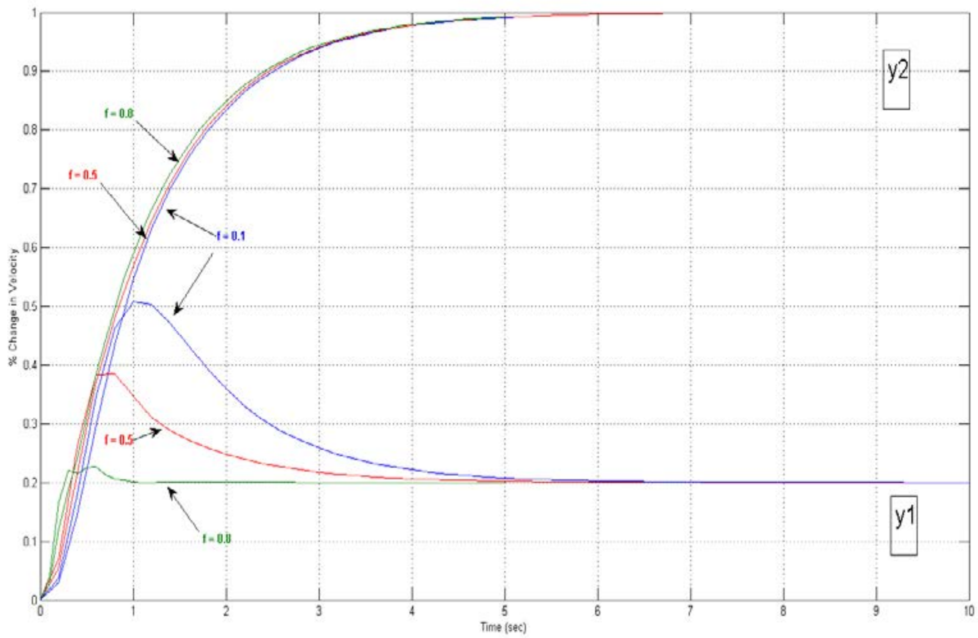

Figure 5.13: Output responses $y_1(t)$ and $y_2(t)$ following a step input of unity on ventilation vane angle for f =0.1, 0.5 and 0.8.

It can be seen that Velocity in the casing section $y_2(t)$ reaches steady state in 6 seconds with almost zero steady state error.

Good damping characteristics with no oscillatory behavior or overshot has been achieved. By increasing f little change in the response speed or settling time was achieved.

The velocity response in the working section $y_1(t)$ also reach steady state within 6 seconds and almost zero steady state errors but with high over shoot especially with low f values.
When higher f values are chosen (i.e. = 0.8), this will decrease the over shoot to about less than 20% as well as given settling time and rise time improvements.

5.5 Disturbance Rejection

To investigate impact of the outer loop feedback gain on the system disturbance rejection, a step input of unity on both disturbances respectively, will be study within selected f values (0.1, 0.5 and 0.8).

By setting two inputs $r_1$and r_2= 0 as well as the second disturbance, the system responses are shown in figure 11.

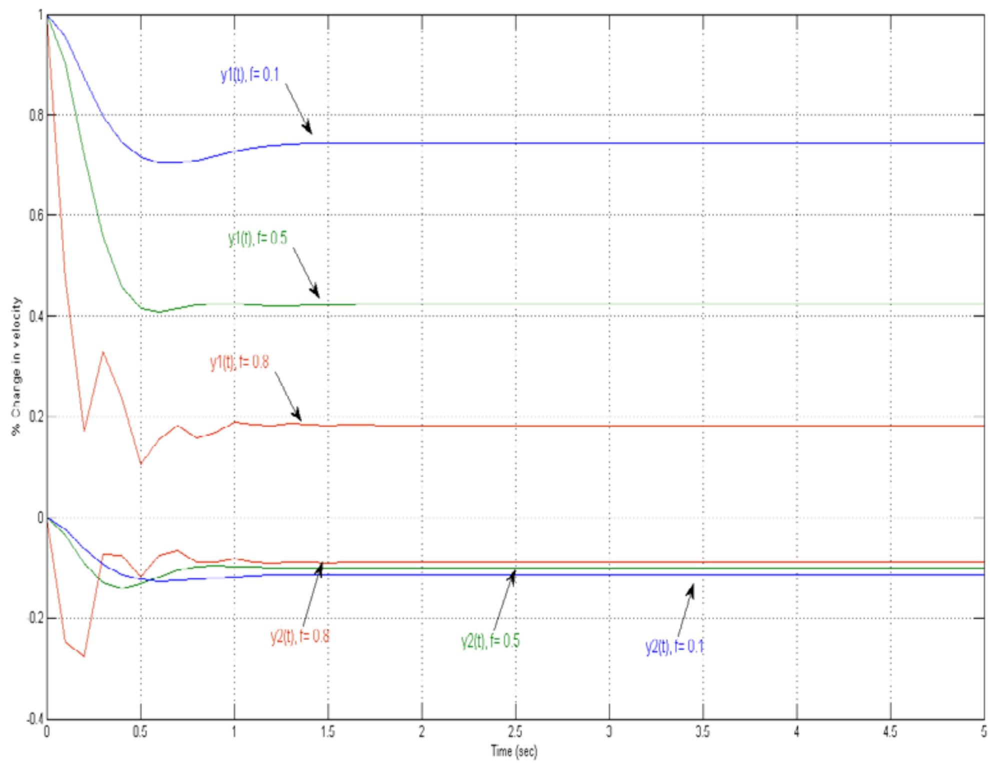

Figure 5.14: System response with a unit step change on $\partial 1$.

It might be evidently shows in figure (5.11) that increasing the outer loop gain, Rises the disturbance recovery and responses.

For first output y_1 (velocity in working section) at low values of f = 0.1 and 0.5, it can be noted weak disturbance recovery percentage (about 25% and 40% respectively).

But with $f = 0.8$ this result in better disturbance recovery rate (more than 80%) and settling time almost a second output y_2 (velocity in casing section) responses have very small effects in disturbance recovery and settling time almost less than a second, then it could be neglected.

Now by keeping two inputs r_1& r_2= 0 and set the first disturbance = 0, with a step input of unity on second disturbance, the system responses are shown in figure (5.15)

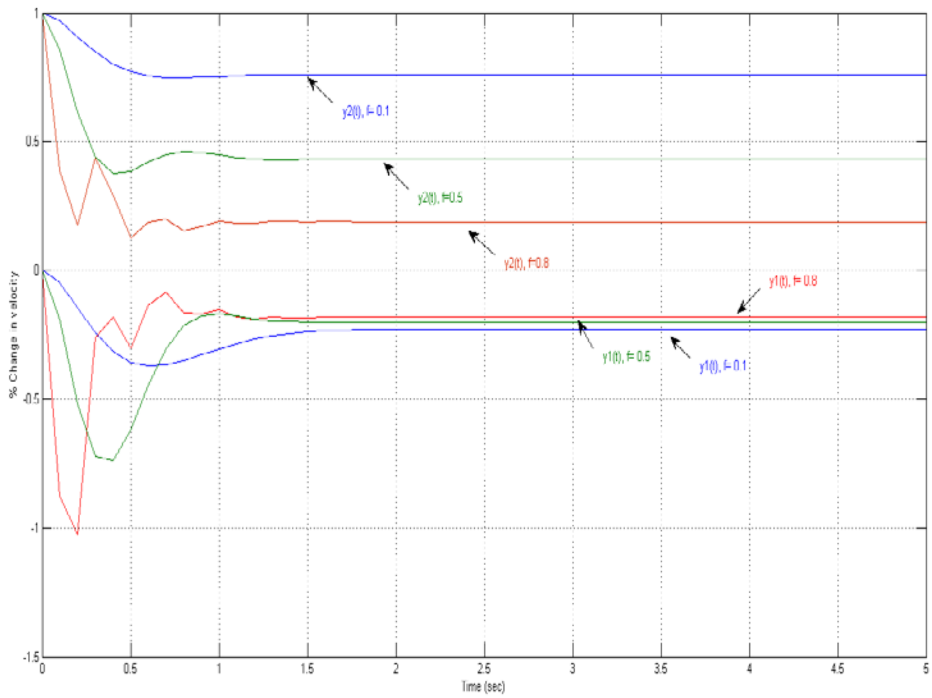

Figure 5.15: System response following a unit step change on ∂2.

Like pervious case it can be shown in figure above that by surging feedback gain for outer loop, would outcome in faster with better disturbance recovery responses (almost more than 80% with f= 0.8 at second output y_2). The first output y_1 could be neglected too.

5.6 Energy Dissipation at different feedback gains

The energy disbursed thru the controller might be calculated using equation below:

$E(t) = \int_0^T \left(u_1{}^2(t) + u_2{}^2(t)\right)dt$ **5.18**

Figure (5.16) displays the energy expended by the control system, following a random disturbance on the two disturbances for the both outputs with
f = 0.1, f = 0.5 and f 0.8.

It can be noted from this plot, when rising values of f, the control energy surges quickly.

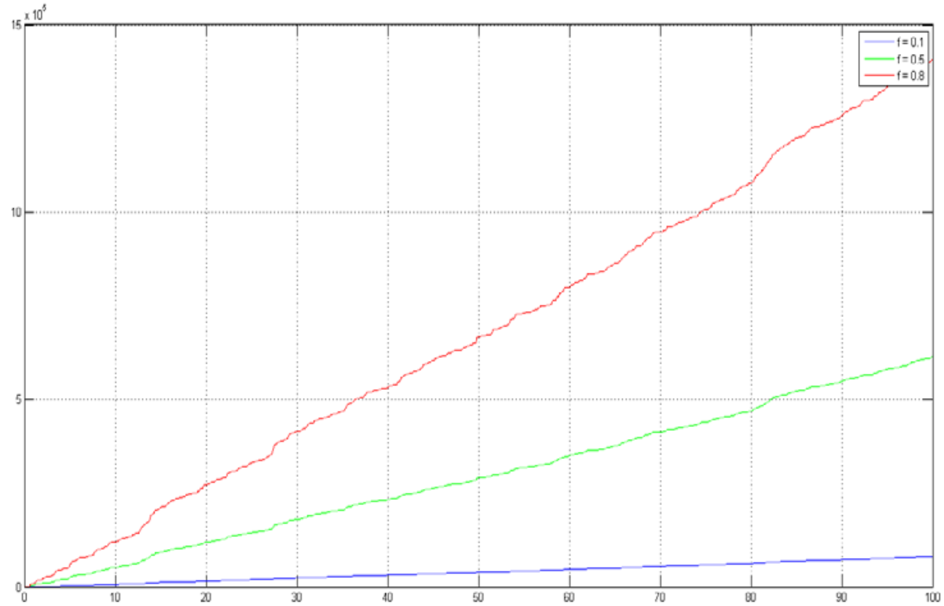

Figure 5.16: Control Energy with random disturbances.

At the end of this chapter it could be concluded that selecting outer loop feedback gains between 0.1 and 0.8 and analyzing effects of that values is necessary to design Least Effort Control so as to accomplish the best closed loop response.

It can be seen with different values of f the system response are acceptable with good settling and rise time eliminating any steady state errors with minimum overshoot.
Also by increasing the value of f, the system performance and response improved and disturbance rejection capacity increases. So f =0.8 is chosen for illustration proposes.

Chapter 6: Interactions Analysis and Diagonal Dominance

Large loop interactions can lead to poor quality of control due to lack of coordination between the two control loops in wind tunnel system. Any change in either of the inputs will lead to a change in the values of both of the outputs. So the first step is to check the interaction level and stability in the wind tunnel arrangement then design of a controller to further reduce the interaction.

6.1 Nyquist Array Method

In Nyquist array method when the closed loop system design reduces independent single loop designs and this occurs when the system transfer function is diagonally dominant.
The Nyquist Array for equation (4.9) could be schemed thru implementing specific matlab commands (written in the Appendix B) to generate the Nyquist diagram, with Gershgorin circles superimposed.

The Gershgorin's bands for the first row of $G(s)$ were applied for the Nyquist diagram of the g_{11} in figure (6.1). It can be noticeably realized that no any bands contain the origin, therefore, the system is diagonally dominance.

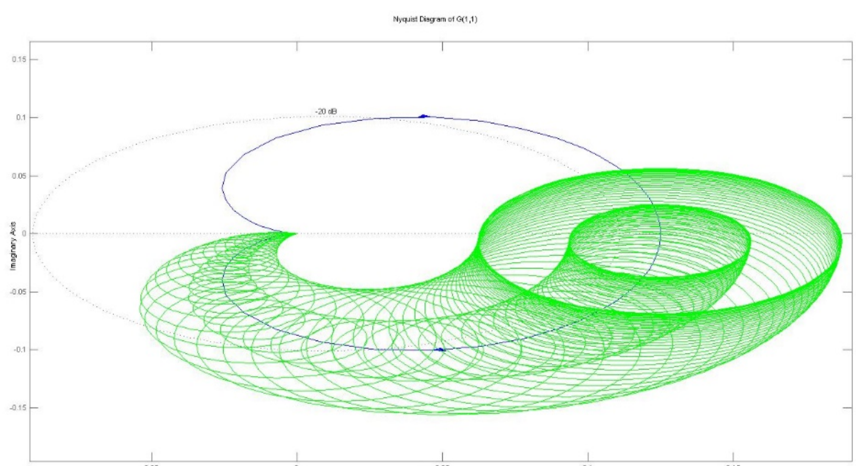

Figure 6.1: Nyquist diagram of g_{11} with Gershgorin's bands

From figure (6.2), Gershgorin's bands for the second row of the element g_{22}, shows bands include the origin of the complex plane, hence the system is not column dominant.

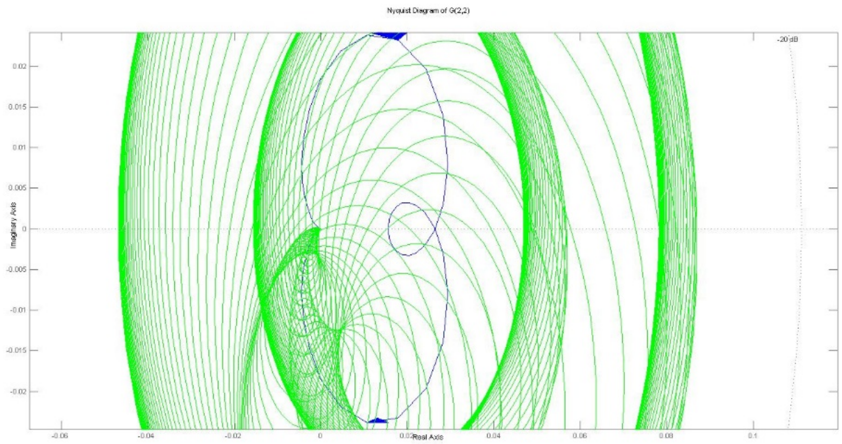

Figure 6.2: Nyquist diagram of g_{22} with Gershgorin's bands

6.2 Design of a controller for interaction minimizing

The first step in planning is interface the plant $G(s)$ with a pre-compensator $K(s)$, so to decrease interaction between the loops and Achieve diagonal dominance.

Controllability and Resiliency analysis should be used to for help developing a pre-compensator and choose controller pairing, there are some model-based tools which helpful in the choice such as the relative gain array (RGA), the relative interaction array, condition number and niederlinski index.

Relative Gain Array (RGA):

From the equation (3.1) and the wind tunnel transfer function matrix and by using (m.file) in Matlab, the resulting matrix for the system is:

$$\underline{\underline{\lambda}} = \begin{bmatrix} 0.5 & 0.5 \\ 0.5 & 0.5 \end{bmatrix}$$

this means strong interaction exists in the system and it does not matter which ever pairing is resorted to.

The relative interaction array

According to the equation (3.2) and wind tunnel transfer function matrix and by using (m.file) in Matlab, the resulting matrix for the system is:

$$\varphi = \begin{bmatrix} 1 & 1 \\ 1 & 1 \end{bmatrix}$$

Which mean there is interaction and pairing is invalid for both loops.

Condition number:

By using Matlab, the Condition Number for the system has been calculated and it is equal to 5.1171 for both diagonal pairing and off diagonal pairing, which mean the system is Well-conditioned.

Niederlinski Index:

The Niederlinski Index can then be calculated from equation (3.5):

For diagonal pairing the NI= 1.5,
then when flipping the pairing the NI = 2.

These values denote that the system has mild interaction and can be integrally stable.

From information and data above it shown that it will be difficult to a design cascade compensator due to high interaction in the system and couldn’t neglect the coupling because the strength of the coupling is high which maximize the risk of poor performance. Further multi-loop control would not effective in reaching the desired specifications.

6.3 Decoupling

In this Dissertation the decoupling method is used, as possible strategy to reduce control loop interaction by adding additional controllers called decouplers.

Decoupling controllers are designed using two process models:

- transfer function model or Dynamic Decoupling which boost the feedback controller with a dynamic block prepared to remove the effect of interactions mathematically

  So to cancel out the effect of u2 on y1 then designed decupler is:

$$T_{12}(s) = -\frac{G_{P12}(s)}{G_{P11}(s)}$$

  Similarly, to cancel the effect of u1 on y2 required decupler is:

$$T_{21}(s) = -\frac{G_{P21}(s)}{G_{P22}(s)}$$

But by using this Decupling model, the designer will face disadvantages and obstacles in the system because they are complex requiring thereby an accurate process model.

Also decupling elements maybe unrealizable if time delays are present, especially with wind tunnel systems when the induction motor delay ascends due to the slip condition variation, by way of the motor speed is altered.

- Steady-State model or Gain Decoupling which Select a model to decouple the system only at steady-state, to reduce complexity and eliminate steady-state interactions, the using of gain decoupling will be best solution.

  Steady-State Decoupler are merely gains:

$$D = G^{-1}(0)\, P$$

where

$$P = \begin{bmatrix} g_{11}(0) & 0 \\ 0 & g_{22}(0) \end{bmatrix}$$

From the wind tunnel transfer function matrix it can be assume the gain decouples are:

$$T_{12} = -\frac{g_{12}(0)}{g_{11}(0)}$$

$$T_{21} = -\frac{g_{21}(0)}{g_{22}(0)}$$

The closed-loop system with gain Decoupling blocks diagram can be constructed as shown in figure (6.3).

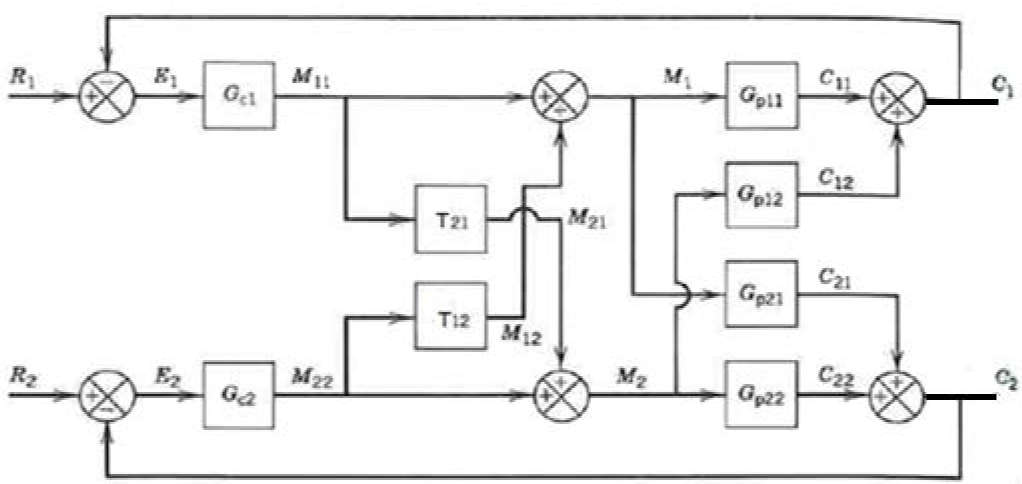

Figure 6.3: The closed-loop system with gain Decoupling blocks diagram

The Gershgorin's bands for the first column of $G(s)$ were applied. It can be clearly seen that none of the bands include the origin, further more it give narrowing circle. So diagonally dominance of the system has been achieved.

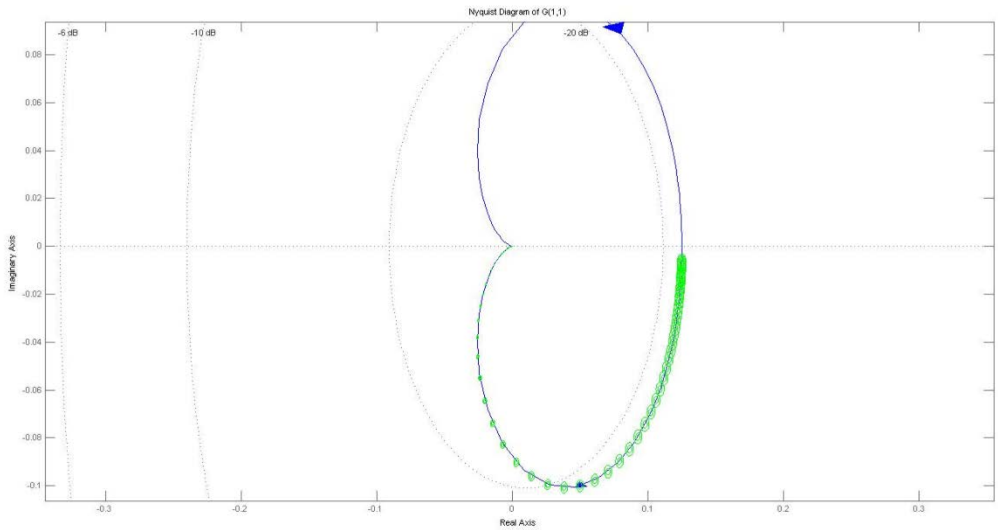

Figure 6.4: The Gershgorin's bands for the first column of $G(s)$

Similarly, Gershgorin's bands for the second column of the element g_{22}, displays not any of the bands contain the origin, hence, diagonally dominance of the system is fully achieved.

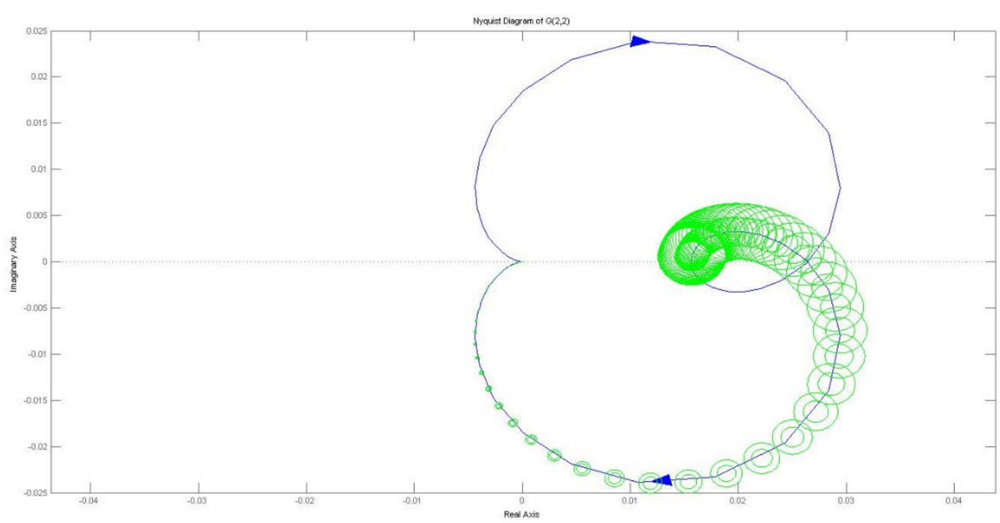

Figure 6.5: The Gershgorin's bands for the second column of $G(s)$

6.4 Output Responses

Second step after diagonal dominance is achieved, is designing a controller for each loop to produce desired closed-loop performance. With unity feedback for each element, their response has been simulated as two separated systems and the simulation model is shown in Appendix (A).

Following a unit step with gain set to 5 to give parity for the first loop and with a proportional plus integral controller was sufficient for the system to eliminate the steady state error resulting from proportional controller.

For the second loop a PID controller was required due to the high order transfer function and to eliminate the overshoot and the oscillations occurring in the output response of the system.

By using the automatic tuning option of MATLAB-Simulink to configure the PI and PID, the parameters and performance are shown in Table (6.1):

Controller	**Controller parameters**				**Performance**		
	P	I	D	Filter coefficient	Rise time (sec)	Settling time (sec)	Overshoot %
PI	0.76	4.48	0	100	1.05	4.03	5.75
PID	58.98	171.3	2.95	17.98	0.2	1.57	6.1

Table 6.1: Controller parameters and performance

With these controllers and unity feedback, the closed loop response followed by step input at the Wind Tunnel system set points were simulated as presented in figures below.

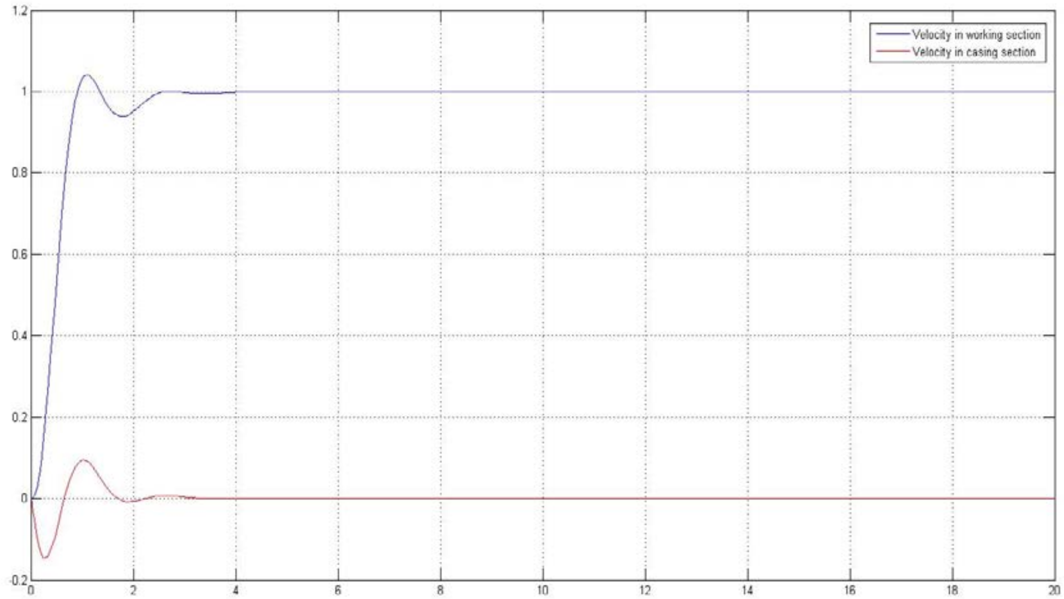

Figure 6.6: Closed Loop Response with a Unit Step on first input

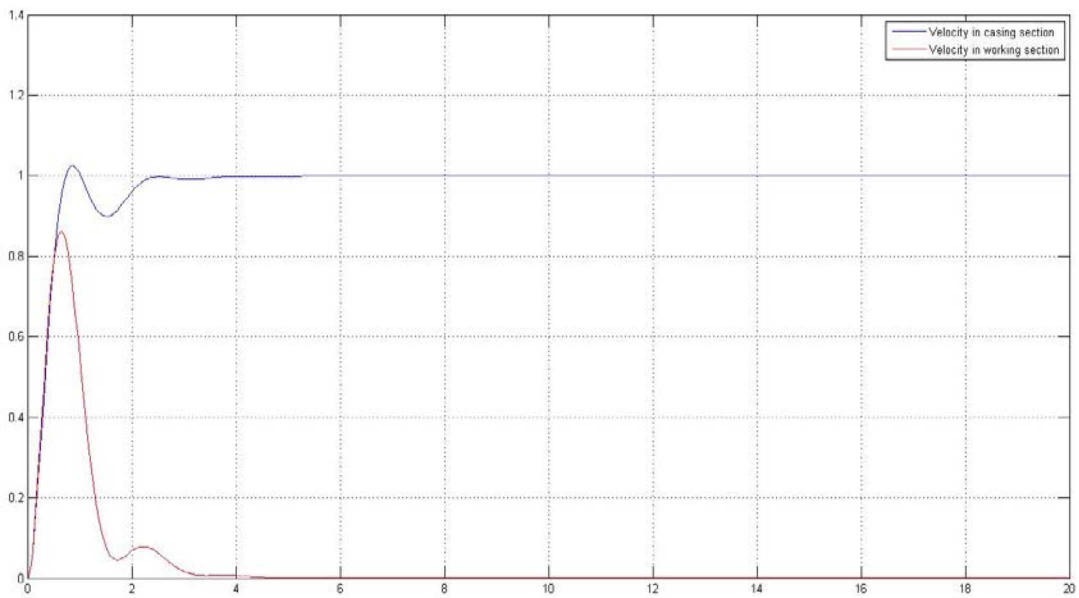

Figure 6.7: Closed Loop Response with a Unit Step on second input

From first figure, it might be realized that the system response is decent with a rise time around 1 sec. and settling time roughly 3 second (damping oscillation). There is no steady state error and minimum overshot.
Also the second output response has acceptable response which disappears after 3 seconds to become zero. This means that system is completely decoupled in steady state.

From second figure, the response is similar to first output response. At the same time, the second output response has a high dynamic reaction but which disappear in 3 seconds to become zero.

6.5 Disturbance Rejection

The responses of the closed-loop system, following step disturbances at both outputs with setting inputs to zero, are shown in figures below respectively.

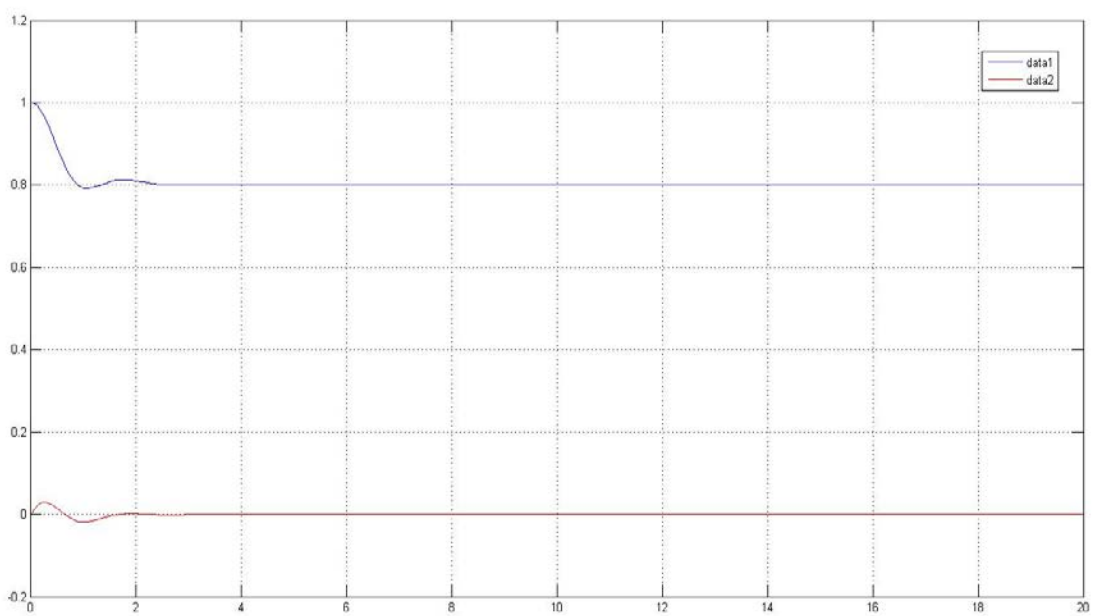

Figure 6.8: System response with a unit step on ∂1

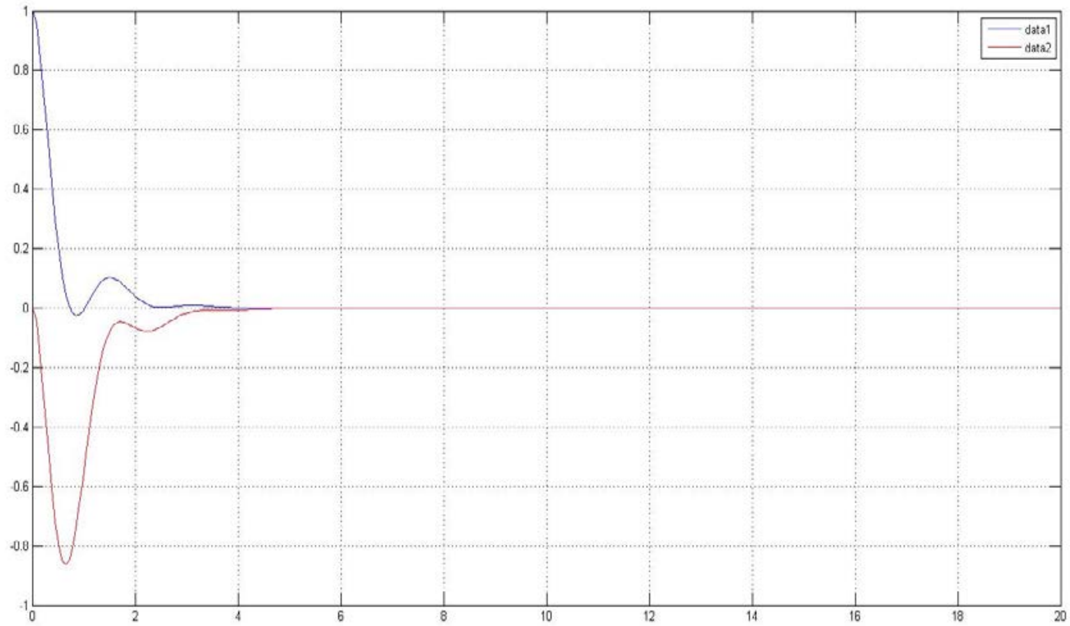

Figure 6.9: System response with a unit step on ∂2

It can be seen from figures that the disturbance rejection for first output is around 20% which is poor. And it is zero response for second output. From second figure it shown minimal oscillation for both output which lead to zero response within 4 seconds.

Chapter 7: Comparative Study and Discussion

This chapter includes a detailed comparative study between techniques used for designing a multivariable controller, includes the main difference in the output response and performance for two techniques which are analyzed and explained in previous chapters. Also the difficulties, advantages and disadvantage will be discussed.

7.1 System Responses and Performance

It is obviously seen, from closed loop responses for the two controller that Least Effort Control outcome is the best matched to decouple compensator.

As shown in output response figures in pervious chapters, with using the least effort controller and for a step input on motor speed at $\boldsymbol{f} = 0.8$, the Velocity response in the working section is without overshot and no oscillatory behavior. Also reaches its steady state in almost 3 seconds with zero steady state error.
The velocity in casing section reaching steady state with interaction limited to 10% within one second.

For output responses with a step input on ventilation vane angle, that Velocity in the casing section reaches steady state in 6 seconds with almost zero steady state error and no overshoot.
The velocity response in the working section also reach 20% output coupling within 2 seconds.

On the other hand, for decoupler compensator the system response for first and second output have 5% overshoot with little oscillatory behavior, and required more than 4 to 6 seconds for reaching steady state.
The interaction disappears within 4 seconds for both outputs but it has high overshoot (around 80%) in the second outputs.

7.2 Disturbance Rejection

The least effort controller for two outputs effects in the greatest disturbance recovery responses. It improve around 80 percent of disturbance with less than 2 seconds, through partial interaction of second output (about 10 percent).

The decoupler compensator for first output recover about 20 percent of disturbance within 3 seconds, and diminished interaction of the velocity in casing section. For the second output it recovers 100 percent of disturbance within 4 seconds for the velocity response in the working section and casing section.

7.3 Energy Dissipation

Simulation models could be created according to equation (5.18). Subsequent a random disturbance on two outputs for 600 seconds, the energy which is expended by different controller might be figured as seen below.

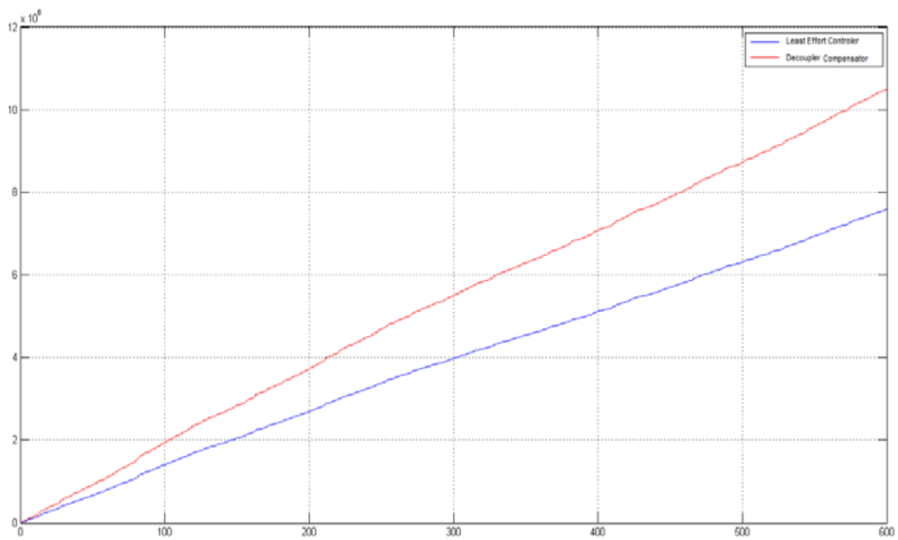

Figure 7.1: Energy Consumed by Least Effort and Decoupler Compensator

It is clearly seen from figure (7.1), the Least Effort Controller expend the least energy.

That might return on the reliability improvment of the wind tunnel because there would be least actuator activity and slightest wear, so will effect noise and heat generation which outcome with minor charges in maintenance.

7.4 Designing and Applying Difficulties

In the least-effort approach, is mandatory signified by its transfer function. The controller consist of two loops. The inner guarantees stable progression, though the outer delivers indicated disturbance suppression situations and affords stated steady state output decoupling. This reflects the flexibility of its design viewpoint, giving freedom to enhance the performance and the closed loop response of multivariable systems. This approach is based upon minimizing the control effort required which is imperative determination necessity.

By using the Nyquist array method, the primary trouble lies on accomplishing the diagonal dominance and selecting proper pre-compensators, with a specific end goal to reduce the system coupling. The diagonal dominance of a specified matrix might be tested graphically by Gershgorin bands superimposing.

The purpose behind this trouble is the absence of a standard technique which can be applied effectively on all application. In this research many Controllability analyses obtained to study the interaction in the system and then checked several techniques to design the pre-compensators, adding to that find suitable controller such as PID controller to tune the output responses.

Chapter 8: Conclusion and Future work

8.1 Conclusion

It can be concluded that:

- The least effort controller's responses are stable and well performed with a simple feedback regulation strategy and flexibility to improve the closed loop response output performance. The illustrative study shows that the theoretical procedures outlined for least effort control are easily exercised.

- In the Least effort control strategy, the difference in the maximum and minimum of the performance index was targeted to ensure the best choice of the gain ratio which minimize energy consumption.

- The least effort controller succeed in reducing the output coupling and diminished interaction with good disturbance rejection acting in the wind tunnel system than decoupling compensator.

- Least effort control strategy is based upon reducing the control effort required, by using less energy, increase the efficiency of operation and improve response of the system, which results in low operational charges.

- Nyquist controller included in this research as a second option to control the system, but the Least Effort Controller fulfilled whole study aims. Which verified she Least Effort approach is better amongst other controllers.

8.2 Future work and Research

1. Future work may include applying alternative control strategies to this wind tunnel arrangement for purpose of comparison.
2. Implementation of a digital compensator to remove or reduce the unwanted noise present in fan motor.

References

- Y Zhu, Faculty EE, Eindhoven University of Technology, Multivariable System Identification for Process Control, Elsevier Science, 2001.

- L Ljung: System Identification - Theory for the User, Prentice-Hall, Englewood Cliffs, N J, 1999 ISBN 0-13-881640, 519 pages.

- Albertos Pérez, P Sala, Antonio, Multivariable control systems : an engineering approach, London : Springer, c2004

- Whalley, R and Ebrahimi, M, “Multivariable System Regulation with Minimum Control Effort”, Proc. IMechE, Part I: Journal of Mechanical Engineering Science, Vol 213, No.16, pp 505 – 514, 1999.

- Whalley, R and Ebrahimi, M, "Process control with minimum control effort", Proceedings of the Institution of Mechanical Engineers Part E Journal of Process Mechanical Engineering, 1999.

- Whalley, R and Ebrahimi, M, "Optimum wind tunnel regulation", Proceedings of the Institution of Mechanical Engineers Part G Journal of Aerospace Engineering, 2001.

- Whalley, R and Ebrahimi, M, "Optimum Multivariable Wind Tunnel System Control", Proceedings of the Institution of Mechanical Engineers Part I Journal of Systems and Control Engineering, 2005.

- Nyquist, H.(1932). Regeneration Theory.Bell System Technical Journal, vol.11,pp.126-147.

- Gerschgorin,S.(1931). Über die Abgrenzung der Eigenwerteeiner Matrix.Izv.Akad.Nauk.USSR Otd.Fiz.-Mat. Nauk 7, pp.749–754.

- R Whalley and D Mitchell,The identification of engineering system parameters,Proceedings of the Institution of Mechanical Engineers, Part I: Journal of Systems and Control Engineering February 1, 1997 vol. 211 no. 1 1-14

- Maciejowski,J.M.(1989).Multivariable Feedback Design. Addison-Wesley Publishing Company

- V. Strejc, System Structure and Control,reprints of the IFAC Workshop, Prague, Czechoslovakia, 3–5 September 1992, ISBN: 978-0-08-042057-8

- Rosenbrock, H.H., "Design of multivariable control systems using the inverse Nyquist array", No.11, pp 1929-1936, 1969.

- B. Veroemen, "Model predictive control of gas turbine installation," WFW Report, 1997

- Munro, N., "Multivariable systems design using the inverse Nyquist array", UMIST, Manchester, 1972.

- Aström, K.J., Albertos, P., Blanke, M., Isidori, A., Schaufelberger, W., Sanz, R., Control of Complex Systems, Springer-Verlag London Limited, 2001.

- V.L. Kakate1, D S Chavan2, P.B Karandikar3 , Niraj Mahulkar, Study of Measurement and Control Aspects of Wind Tunnel, INTERNATIONAL JOURNAL OF INNOVATIVE RESEARCH IN ELECTRICAL, ELECTRONICS, INSTRUMENTATION AND CONTROL ENGINEERING, Vol. 2, Issue 3, March 2014

- National Aeronautics and Space Administration, NASA. http://www.nasa.gov/centers/langley/news/factsheets/windtunnels.html

- "Wind Tunnels of NASA" by Donald D. Baals and William R. Corliss.
- Wind Tunnel from Wikipedia, the free encyclopedia. https://en.wikipedia.org/wiki/Wind_tunnel

- Tabrej khan, Wind tunnel Experiments procedure In UPM, Malaysia, University Putra Malaysia, Faculty of Engineering, Graduate Student.

- P Albertos Pérez; R Strietzel; N Mort; Control engineering solutions : a practical approach, London : Institution of Electrical Engineers, ©1997.

- Ichikawa & Furuta , Advances in Control Education, 1st Edition, Pergamon,1994.

- Edmunds, J.M. and Murno,N , Design Techniques in the Frequency Domain, Control System, Robotics and Automation, Vol 3.

- N. AL-Hatmi, Ming T Tham, CONTROLLABILITY AND RESILIENCY ASPECTS OF GRAVITY THREE-PHASE HORIZONTAL SEPARATORS, January 2006.

- Ajayi T.O. and I.S.Ogboh, Determination of Control Pairing for Higher Order Multivariable Systems by the use of Multi-Ratios, International Journal of Scientific & Engineering Research Volume 3, Issue 3, March -2012.

- S. Akraminejad, M. R. Hojjati, M. Razmdideh, A. Shokrgu, Decentralized Control Structure Design A Case Study, Recent Researches in Circuits, Systems, Control and Signals

APPENDIX A

Simulation Models:

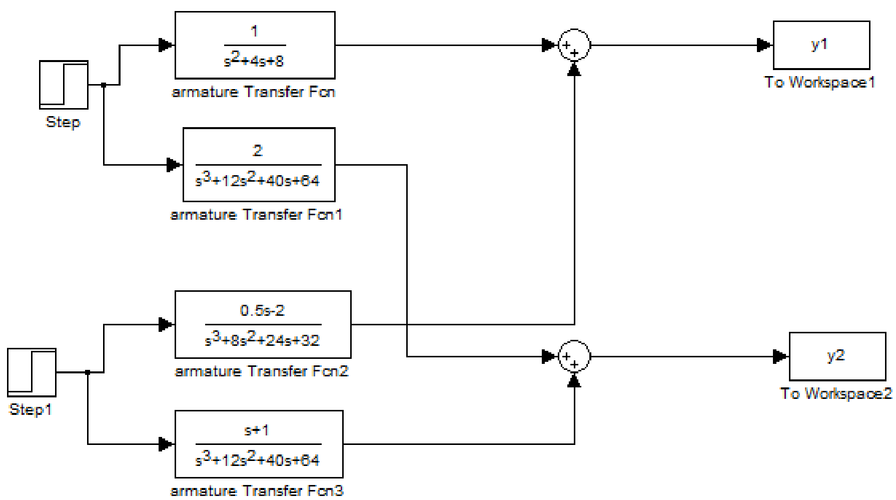

Figure A.1, General Open Loop Simulation Model

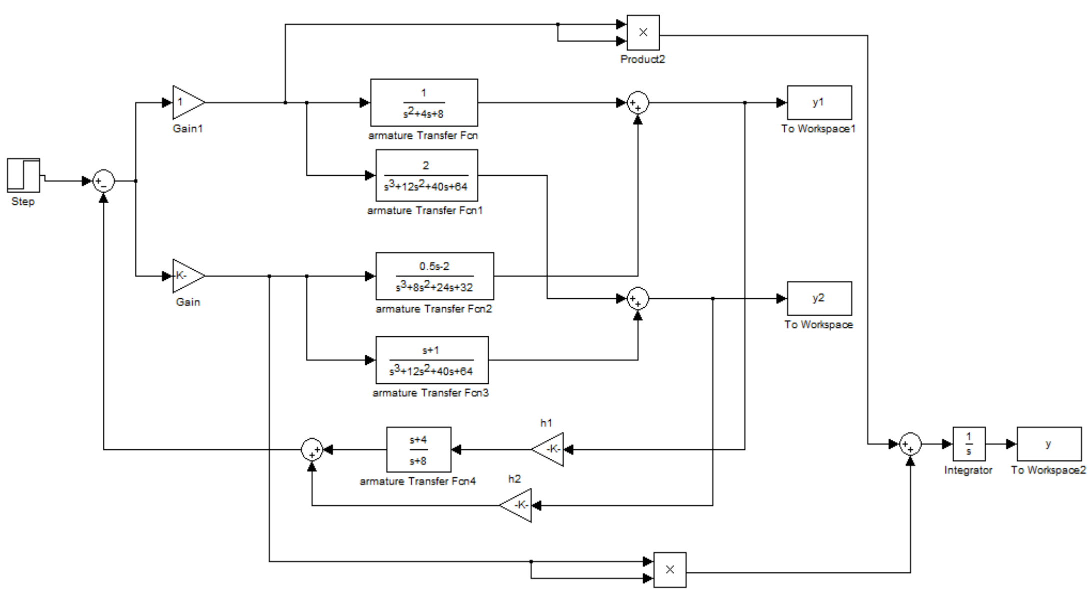

Figure A.2, Inner loop system block diagram.

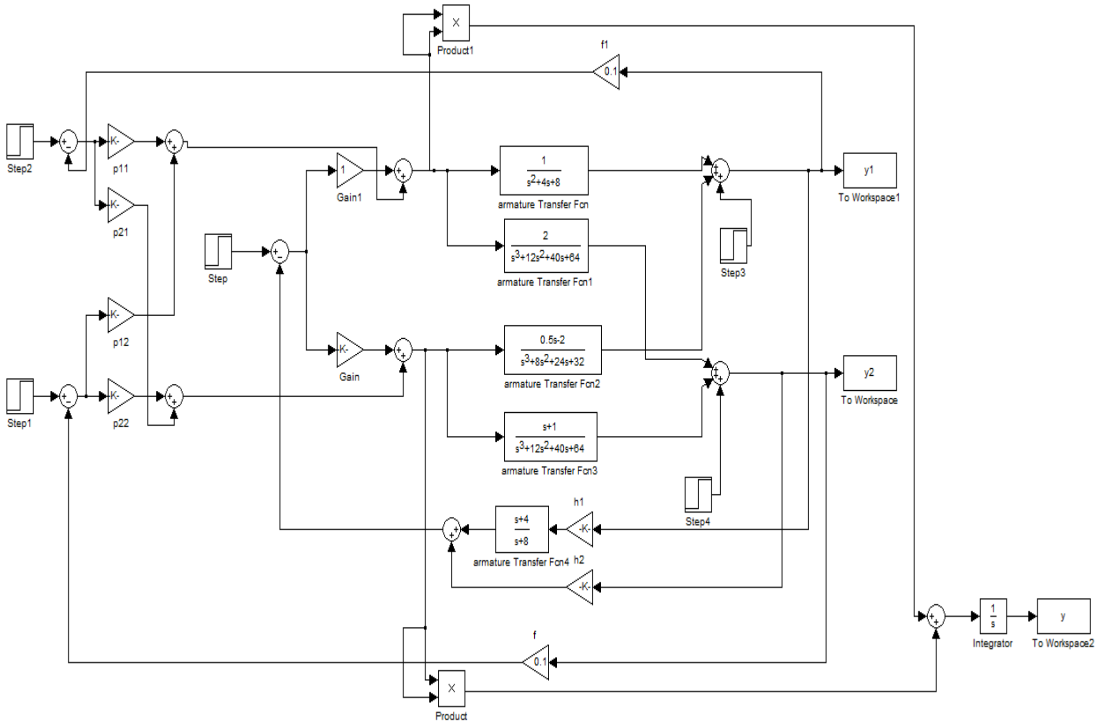

Figure A.3, Outer loop system block diagram

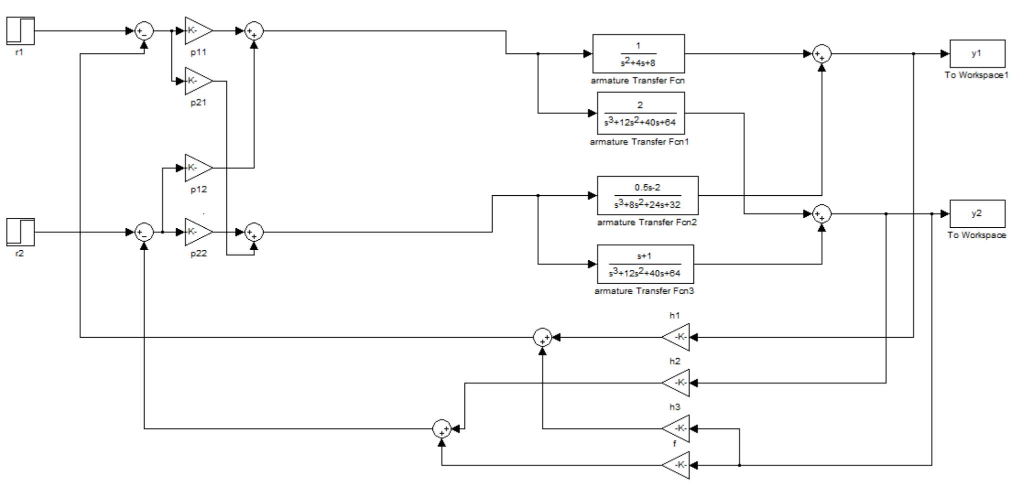

Figure A.4, Conventional block diagram.

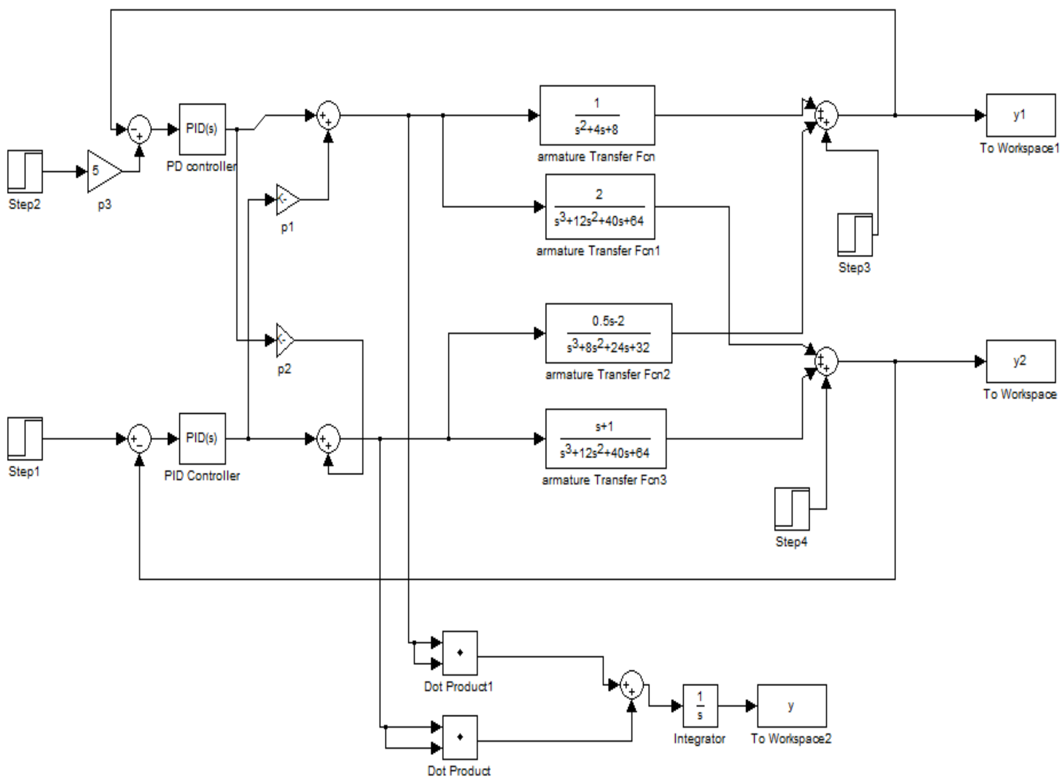

Figure A.5, Closed Loop by Nyquist Array Method Simulation Model

APPENDIX B

A Program in Matlab for Building Gershgorin circles:

```
g11=tf([1],[1 4 8]);
g22=tf([1 1],[1 12 40 64]);
g12=tf([-0.5 2],[1 8 24 32]);
g21=tf([2],[1 12 40 64 ]);
G=[g11 g12;g21 g22]
G=[g11 g12;g21 g22]
A= [0.5 0.25;-1 0.5]
Q=G*A
```

```
function gershband(a,b,c,d,e)
%GERSHBAND - Finds the Gershorin Bands of a nxn LTI MIMO SYS model
% The use of the Gershorin Bands along the Nyquist plot is helpful for
% finding the coupling grade of a MIMO system.
%
% Syntax: gershband(SYS) - computes the Gershgorin bands of SYS
%         gershband(SYS,'v') - computes the Gershgorin bands and the
%                              Nyquist array of SYS
% Inputs:
%    SYS - LTI MIMO system, either in State Space or Transfer Function
%    representation.
%
%
%
%
%
%
%
%
%
%
%
%
%
```

```
%
% Example:
%    g11=tf(2,[1 3 2]);
%    g12=tf(0.1,[1 1]);
%    g21=tf(0.1,[1 2 1]);
%    g22=tf(6,[1 5 6]);
%    G=[g11 g12; g21 g22];
%    gershband(G);
%
% Other m-files required: sym2tf, ss2sym
% Subfunctions: center, radio
% See also: rga
%
% Author: Oskar Vivero Osornio
% email: oskar.vivero@gmail.com
% Created: February 2006;
% Last revision: 11-May-2006;

% May be distributed freely for non-commercial use,
% but please leave the above info unchanged, for
% credit and feedback purposes

%------------- BEGIN CODE --------------
%--------- Determines Syntax -----------
ni=nargin;

switch ni
    case 1
        %Transfer Function Syntax
        switch class(a)
            case 'tf'
                %Numeric Transfer Function Syntax
                g=a;

            case 'sym'
                %Symbolic Transfer Function Syntax
                g=sym2tf(a);
        end
        e=0;
    case 2
        %Transfer Function Syntax with Nyquist Array
        switch class(a)
            case 'tf'
                %Numeric Transfer Function Syntax
                g=a;

            case 'sym'
                %Symbolic Transfer Function Syntax
                g=sym2tf(a);
        end
        e=1;

    case 4
        %State Space Syntax
        g=ss2sym(a,b,c,d);
```

```
        g=sym2tf(g);
        e=0;
    case 5
        %State Space Syntax
        g=ss2sym(a,b,c,d);
        g=sym2tf(g);
        e=1;
end
%---------------------------------------
[n,m]=size(g);
w=logspace(-1,6,200);
q=0:(pi/50):(2*pi);

for i=1:n
    for j=1:m
        if i==j
            figure(i)
            nyquist(g(i,i));
            grid on
            title(['Nyquist Diagram of G(',num2str(i),',',num2str(j),')'])
            for iest=1:n
                for jest=1:m
                    if iest~=jest
                        hold on
                        C=center(g(i,j),w);
                        R=radio(g(iest,jest),w);
                        for k=1:length(C)

plot((R(k)*cos(q))+real(C(k)),(R(k)*sin(q))+imag(C(k)),'g-')
                        end
                        hold off
                    end
                end
            end
        end
    end
end

if e==1
    figure(n+1)
    nyquist(g);
    grid on
end
%------------ Subfunction --------------
function C = center(g,w)
g=tf2sym(g);
C=subs(g,complex(0,w));

function R = radio(g,w)
g=tf2sym(g);
R=abs(subs(g,complex(0,w)));
%------------- END OF CODE --------------
```

Mathematics Equations calculation by Maple software:

$$b=\begin{bmatrix}2\\1\end{bmatrix}\cdot 16$$

$$Q=\begin{bmatrix}4-2x & 2+x\\ 1+0.5x & x\end{bmatrix}\xrightarrow{\text{inverse}}$$

$$\begin{bmatrix}-\frac{x}{-2.0x+2.5x^2+2} & \frac{2.+x}{-2.x+2.500000000x^2+2.}\\ \frac{1.+0.5000000000x}{-2.x+2.500000000x^2+2.} & \frac{2(-2.+x)}{-2.x+2.500000000x^2+2.}\end{bmatrix}$$

$$Q^{-1}=\begin{bmatrix}-\frac{x}{-2.0x+2.5x^2+2} & \frac{2.+x}{-2.x+2.500000000x^2+2.}\\ \frac{1.+0.5000000000x}{-2.x+2.500000000x^2+2.} & \frac{2(-2.+x)}{-2.x+2.500000000x^2+2.}\end{bmatrix}\xrightarrow{\text{transpose}}$$

$$\begin{bmatrix}-\frac{x}{-2.0x+2.5x^2+2} & \frac{1.+0.5000000000x}{-2.x+2.500000000x^2+2.}\\ \frac{2.+x}{-2.x+2.500000000x^2+2.} & \frac{-4.+2x}{-2.x+2.500000000x^2+2.}\end{bmatrix}$$

$$J=16^2(1+x^2)\begin{bmatrix}2 & 1\end{bmatrix}\cdot\begin{bmatrix}-\frac{x}{-2.0x+2.5x^2+2} & \frac{1.+0.5000000000x}{-2.x+2.500000000x^2+2.}\\ \frac{2.+x}{-2.x+2.500000000x^2+2.} & \frac{-4.+2x}{-2.x+2.500000000x^2+2.}\end{bmatrix}$$

$$\cdot\begin{bmatrix}-\frac{x}{-2.0x+2.5x^2+2} & \frac{2.+x}{-2.x+2.500000000x^2+2.}\\ \frac{1.+0.5000000000x}{-2.x+2.500000000x^2+2.} & \frac{2(-2.+x)}{-2.x+2.500000000x^2+2.}\end{bmatrix}\cdot\begin{bmatrix}2\\1\end{bmatrix}$$

$$\overset{\text{simplify}}{=}$$

$$\frac{2048.\,(1.+x^2)\,(-8.\,x+5.\,x^2+4.)}{(-4.\,x+5.\,x^2+4.)^2}$$

$$J=\frac{2048.\,(1.+n^2)\,(-8.\,n+5.\,n^2+4.)}{(-4.\,n+5.\,n^2+4.)^2}\rightarrow$$

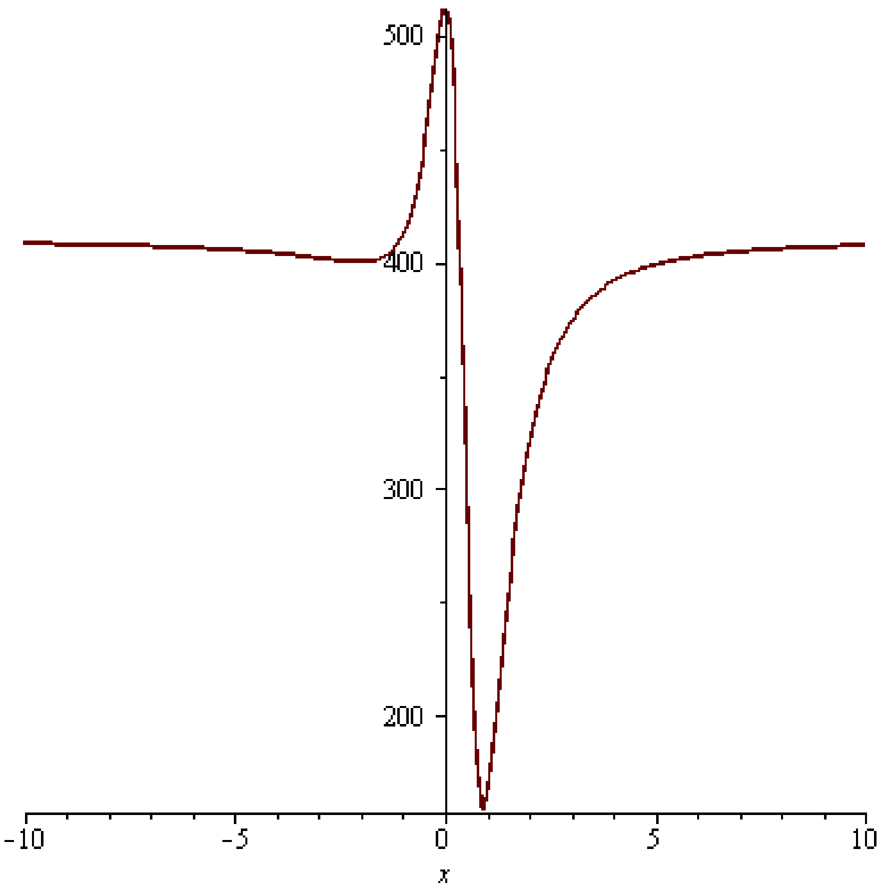

$$\xrightarrow{\text{differentiate w.r.t. x}}=\frac{4096.\,x\,(11.\,x^2+12.\,x-20.)}{(-4.\,x+5.\,x^2+4.)^3}\xrightarrow{\text{solve for x}}$$

[[$x=0.$], [$x=0.9090909091$], [$x=-2.$]]

[[$n=0.$], [$n=0.9090909091$], [$n=-2.$]]

$$\frac{4096.\,n\,(11.\,n^2+12.\,n-20.)}{(-4.\,\mathrm{n}+5.\,n^2+4.)^3}$$

$k1 = 1$

$k2 = 0.9090909091$

$where\ n = .0909$

$$h = \begin{bmatrix} 4 - 2 \cdot 0.9090 & 2 + 0.9090 \\ 1 + 0.5 \cdot 0.9090 & 0.9090 \end{bmatrix}^{-1} \cdot \begin{bmatrix} 2 \\ 1 \end{bmatrix} \cdot 16$$

$$h = \begin{bmatrix} 7.76615232665355 \\ 5.17506209117977 \end{bmatrix}$$

$$\begin{bmatrix} 0.125 & -0.0625 \\ 0.03125 & 0.0156 \end{bmatrix} \xrightarrow{\text{inverse}} \begin{bmatrix} 3.99679743795036 & 16.0128102481986 \\ -8.00640512409928 & 32.0256204963971 \end{bmatrix}$$

$$K(0) = \begin{bmatrix} 1 \\ 0.9090 \end{bmatrix}$$

$$h(0) = \begin{bmatrix} 3.883 & 5.1750 \end{bmatrix}$$

$$K(0) \times h(0) = \begin{bmatrix} 1 \\ 0.9090 \end{bmatrix} \times \begin{bmatrix} 3.883 & 5.175 \end{bmatrix}$$

$$= \begin{bmatrix} 3.883 & 5.175 \\ 3.529 & 4.704 \end{bmatrix}$$

$P =$

$$\left(\begin{bmatrix} 4 & 16 \\ -8 & 32 \end{bmatrix} + \begin{bmatrix} 3.883 & 5.175 \\ 3.529 & 4.704 \end{bmatrix}\right) \cdot \begin{bmatrix} 1 & 0.2 \\ 0.1 & 1 \end{bmatrix} \cdot \left(\begin{bmatrix} 1 & 0 \\ 0 & 1 \end{bmatrix} - \begin{bmatrix} 0.5 & 0 \\ 0 & 0.5 \end{bmatrix} \cdot \begin{bmatrix} 1 & 0.2 \\ 0.1 & 1 \end{bmatrix}\right)^{-1}$$

$$\begin{bmatrix} 25.0523673469388 & 50.5136734693878 \\ 5.67424489795918 & 72.7544489795918 \end{bmatrix}$$

$$\left(\begin{bmatrix} 4 & 16 \\ -8 & 32 \end{bmatrix} + \begin{bmatrix} 3.883 & 5.175 \\ 3.529 & 4.704 \end{bmatrix}\right) \cdot \begin{bmatrix} 1 & 0.2 \\ 0.1 & 1 \end{bmatrix} \cdot \left(\begin{bmatrix} 1 & 0 \\ 0 & 1 \end{bmatrix} - \begin{bmatrix} 0.1 & 0 \\ 0 & 0.1 \end{bmatrix} \cdot \begin{bmatrix} 1 & 0.2 \\ 0.1 & 1 \end{bmatrix}\right)^{-1}$$

$$\begin{bmatrix} 11.3953642874784 & 25.5327858730551 \\ -0.447569770313657 & 39.7787206717708 \end{bmatrix}$$

$$\left(\begin{bmatrix} 4 & 16 \\ -8 & 32 \end{bmatrix} + \begin{bmatrix} 3.883 & 5.175 \\ 3.529 & 4.704 \end{bmatrix}\right) \cdot \begin{bmatrix} 1 & 0.2 \\ 0.1 & 1 \end{bmatrix} \cdot \left(\begin{bmatrix} 1 & 0 \\ 0 & 1 \end{bmatrix} - \begin{bmatrix} 0.7 & 0 \\ 0 & 0.7 \end{bmatrix} \cdot \begin{bmatrix} 1 & 0.2 \\ 0.1 & 1 \end{bmatrix}\right)^{-1}$$

$$\begin{bmatrix} 57.2663591022444 & 102.562967581047 \\ 28.2606733167082 & 132.554314214464 \end{bmatrix}$$

$$\begin{bmatrix} 140.449558823530 & 226.117647058824 \\ 99.4361764705883 & 258.597941176471 \end{bmatrix}$$

$$\left(\begin{bmatrix} 3.996 & 16.0128 \\ -8.0064 & 32.025 \end{bmatrix} + \begin{bmatrix} 3.883 & 5.175 \\ 3.529 & 4.704 \end{bmatrix}\right) \cdot \begin{bmatrix} 1 & 0.2 \\ 0.1 & 1 \end{bmatrix} \cdot \left(\begin{bmatrix} 1 & 0 \\ 0 & 1 \end{bmatrix} - \begin{bmatrix} 0.8 & 0 \\ 0 & 0.8 \end{bmatrix} \cdot \begin{bmatrix} 1 & 0.2 \\ 0.1 & 1 \end{bmatrix}\right)^{-1}$$

$$\begin{bmatrix} 140.464852941177 & 226.189882352941 \\ 99.4772647058824 & 258.749411764706 \end{bmatrix}$$

$$\begin{bmatrix} 11.395 & 25.532 \\ -0.447 & 39.778 \end{bmatrix}^{-1} \cdot \begin{bmatrix} 3.883 & 5.175 \\ 3.529 & 4.704 \end{bmatrix} + \begin{bmatrix} 0.1 & 0 \\ 0 & 0.1 \end{bmatrix}$$

$$\begin{bmatrix} 0.238493403485284 & 0.184531392289843 \\ 0.0902736827230610 & 0.220329969640343 \end{bmatrix}$$

$$\begin{bmatrix} 11.395 & 25.532 \\ -0.447 & 39.778 \end{bmatrix}^{-1} \cdot \begin{bmatrix} 3.883 & 5.175 \\ 3.529 & 4.704 \end{bmatrix} + \begin{bmatrix} 0.5 & 0 \\ 0 & 0.5 \end{bmatrix}$$

$$\begin{bmatrix} 0.638493403485284 & 0.184531392289843 \\ 0.0902736827230610 & 0.620329969640343 \end{bmatrix}$$

$$\begin{bmatrix} 11.395 & 25.532 \\ -0.447 & 39.778 \end{bmatrix}^{-1} \cdot \begin{bmatrix} 3.883 & 5.175 \\ 3.529 & 4.704 \end{bmatrix} + \begin{bmatrix} 0.8 & 0 \\ 0 & 0.8 \end{bmatrix}$$

$$\begin{bmatrix} 0.938493403485284 & 0.184531392289843 \\ 0.0902736827230610 & 0.920329969640343 \end{bmatrix}$$

$$\begin{bmatrix} 0.938493403485284 & 0.184531392289843 \\ 0.0902736827230610 & 0.920329969640343 \end{bmatrix}$$

$$\left(\begin{bmatrix} 140.449 & 226.117 \\ 99.436 & 258.597 \end{bmatrix}^{-1} \cdot \begin{bmatrix} 3.883 & 5.175 \\ 3.529 & 4.704 \end{bmatrix} \right) + \begin{bmatrix} 0 & 0.8 \\ 0.8 & 0 \end{bmatrix}$$

$$\begin{bmatrix} 0.0149011571223237 & 0.819846388584332 \\ 0.807916907544885 & 0.0105591112995447 \end{bmatrix}$$

APPENDIX C

Multivariable system regulation

R Whalley and M Ebrahimi_

Department of Mechanical and Medical Engineering, University of Bradford, West Yorkshire, UK

The manuscript was received on 28 October 2005 and was accepted after revision for publication on 30 January 2006.
DOI: 10.1243/09544062JMES218

1 INTRODUCTION

A novel controller design method for multivariable systems that employs output feedback, passive compensation, and proportional regulation, is outlined in this contribution. The feedback structure proposed for analysis purposes comprises an outer- and an inner-loop configuration enabling output transient, steady state, and disturbance recovery specification aims to be addressed for linear systems having m inputs and outputs.

Operating conditions whereby the principal perturbations entering the system arise from disturbances are acknowledged. When commissioning the system, changing objectives, production schedules, product quality, specifications, tolerances etc., the reference set points may be adjusted. Otherwise, these settings remain invariant for relatively long periods of time, while the regulator suppresses the output excursions arising from disturbance variations.

The use of active elements, such as integrators for this task, has been avoided in the design procedure accommodating thereby applications in which limitations on the space, inertia, and mass of power supplies are mandatory features. This encompasses, for example, aerospace, vehicle, and military systems, as considered by Whalley and Ebrahimi [**1, 2**], where portable units, with strictly restricted power capacity, are employed.

Otherwise, in process systems studies, such as those presented by Whalley and Ebrahimi [**3**], in which pneumatic, hydraulic, and/or electrical supplies may be required, restricted power availability inhibits the use of pure integral action, inviting the inclusion of passive elements, for dynamic and steady-state performance adjustment.

In any case, the dissipation of substantial control effort invalidates important assumptions, where small signal linearization has been used to obtain the system models employed for controller design purposes. Moreover, the safe working range of components is threatened by integral controllers, as this element's corrective action increases monotonically, under sustained error conditions.

The frugal use of control energy is further emphasized in this submission by employing an optimum, least effort, regulation strategy. This design is initially based on the dissipation of the absolute minimum amount of control effort required, commensurate with the attainment of a specified, closed-loop, characteristic equation. Thereafter, to improve

*Corresponding author: Department of Mechanical and Medical Engineering, University of Bradford, Richmond Road, Bradford, West Yorkshire, BD7 1DP, UK. email: m.ebrahimi@bradford.ac.uk

disturbance suppression and reduce output interaction, the control energy expended, with random disturbance changes entering the system, becomes the relative minimum, in respect of the final closed-loop performance criteria to be accomplished.

Associated with the closed-loop system's performance aims of low steady-state output interaction, well behaved transient characteristics, and acceptable recovery responses from disturbance perturbations, are the important measures of relative stability. Relative stability may be established using existing frequency response methods, in the rapid assessment of the safety margins available.

Initially, the design process should be aimed at securing the closed-loop system's dynamic response by means of the inner, feedback loop. Low steady-state output coupling with adequate disturbance recovery are addressed thereafter via pre-compensation and the outer-loop gain settings, respectively.

These objectives are assisted by the proportional influence which the outer-loop feedback gain has on the system's low frequency disturbance suppression properties. The relative stability and frequency response characteristics, are also an indication of the 'trade-off' between these performance measures.

Attaining the final performance specification while dissipating minimum control energy also guarantees least actuator activity. Consequently, operating conditions with minimum wear, maintenance costs, and refit time would be attainable.

Least actuator activity also leads to the generation of least heat, noise, and vibration, all of which are highly desirable operating objectives, worthy of aspiration.

Finally, the implementation procedure available is also attractive. Owing to the simple transformation relationships, a conventional pre- and feedback compensation structure can be employed for implementation purposes, as in references [4, 5] securing thereby cost-effectiveness and operating efficiency.

2 CLOSED-LOOP STRATEGY

In the design procedure outlined herein the outer loop and pre-compensator will, primarily, be employed to secure specified steady state, reference set point, and low frequency, disturbance-output conditions. The inner loop will be utilized to attain initial, targeted, dynamic, and load disturbance recovery rates, where the system equation is

$$\boldsymbol{y}(s) = \mathbf{G}(s)\boldsymbol{u}(s) + \boldsymbol{\delta}(s) \tag{1}$$

The control law for the proposed configuration is

$$\boldsymbol{u}(s) = \boldsymbol{k}(s)(\bar{r}(s) - \boldsymbol{h}(s)\boldsymbol{y}(s)) + \mathbf{P}(\boldsymbol{r}(s) - \mathbf{F}\boldsymbol{y}(s)) \tag{2}$$

where in equations (1) and (2) there are m independent inputs, disturbances, and outputs and

$$\mathbf{F} = \mathrm{Diag}(f_1, f_2, \ldots, f_m), \quad 0 < f_j < 1,\ 1 \leqslant j \leqslant m$$

With $\bar{r}(s) = 0$, the closed- loop equation becomes

$$\begin{aligned} \boldsymbol{y}(s) = {} & (\mathbf{I}_m + \mathbf{G}(s)(\boldsymbol{k}(s) >< \boldsymbol{h}(s) + \mathbf{PF}))^{-1} \\ & \times (\mathbf{G}(s)\mathbf{P}\boldsymbol{r}(s) + \boldsymbol{\delta}(s) \end{aligned} \tag{3}$$

In equation (3), $\|\boldsymbol{G}(s)(\boldsymbol{k}(s) >< \boldsymbol{h}(s) + \mathbf{PF}\|_\infty$ is finite for all s on the D contour.

If a steady-state matrix $\mathbf{S}_s$ is now selected such that

$$\boldsymbol{y}(0) = \mathbf{S}_s\boldsymbol{r}(0)$$

then from equation (3) with $\boldsymbol{\delta}(s)$ null

$$\mathbf{P} = (\mathbf{G}(0)^{-1} + \boldsymbol{k}(0) >< \boldsymbol{h}(0))\mathbf{S}_s(\mathbf{I} - \mathbf{FS}_s)^{-1} \tag{4}$$

where for steady-state decoupling $\mathbf{S}_s = \mathbf{I}_m$. Otherwise, to achieve 'low' steady-state interaction, $\mathbf{S}_s$ would have diagonal elements of unity and off-diagonal elements $|s_{i,j}| \langle\langle 1, 1 \leqslant i, j \leqslant m, i \neq j$. Consequently, specifying steady-state, closed-loop non-interaction and substituting for $\mathbf{P}$ from equation (4) results in equation (3) becoming:

$$\begin{aligned} \boldsymbol{y}(s) = {} & \big\{\mathbf{I}_m + \mathbf{G}(s)\big[\boldsymbol{k}(s) >< \boldsymbol{h}(s) \\ & + (\mathbf{G}(0)^{-1} + \boldsymbol{k}(s) >< \boldsymbol{h}(s))(\mathbf{I}_m - \mathbf{F})^{-1}\mathbf{F}\big]\big\}^{-1} \\ & \times \{\mathbf{G}(s)\mathbf{P}\boldsymbol{r}(s) + \boldsymbol{\delta}(s)\} \end{aligned} \tag{5}$$

at low frequencies, as shown in Appendix 1

$$\mathbf{G}(s)\mathbf{P} \cong \frac{1}{1-f}(\mathbf{I}_m + \mathbf{G}(s)\boldsymbol{k}(0) >< \boldsymbol{h}(0))$$

Consequently, equation (5), on approaching steady-state conditions becomes

$$\boldsymbol{y}(s) = \mathbf{I}_m\boldsymbol{r}(s) + \mathbf{S}(s)\boldsymbol{\delta}(s) \tag{6}$$

where the low frequency sensitivity matrix

$$\mathbf{S}(s) = (1-f)(\mathbf{I}_m + \mathbf{G}(s)\boldsymbol{k}(s) >< \boldsymbol{h}(s))^{-1},\ 0 < f < 1.0$$

Evidently, from equation (6), steady-state, non-interaction following reference input changes will be achieved. Moreover, as f is increased, $f < 1$, there will be increasing steady-state disturbance rejection, provided stability can be maintained.

It is also evident from equation (3) that since a conventional multivariable regulator structure comprising a forward path $\mathbf{K}(s)$ and feedback path compensator $\mathbf{H}(s)$ are required for implementation purposes, then these matrices can easily be computed from the closed-loop equation

$$\boldsymbol{y}(s) = (\mathbf{I}_m + \mathbf{G}(s)\mathbf{K}(s)\mathbf{H}(s))^{-1}[\mathbf{GK}(s)\boldsymbol{r}(s) + \boldsymbol{\delta}(s)] \quad (7)$$

On comparing equations (3) and (7), evidently

$$\mathbf{K}(s) = \mathbf{P} \quad (8)$$

and

$$\mathbf{K}(s)\mathbf{H}(s) = \boldsymbol{k}(s) >< \boldsymbol{h}(s) + \mathbf{PF}$$

hence

$$\mathbf{H}(s) = \mathbf{P}^{-1}\boldsymbol{k}(s) >< \boldsymbol{h}(s) + \mathbf{F} \quad (9)$$

enabling the employment of established feedback structures.

From equations (8) and (9), it is clear that the compensators $\mathbf{K}(s)$ and $\mathbf{H}(s)$ are constant and full rank $m \times m$ matrices, respectively. The feedback matrix $\mathbf{H}(s)$ is, moreover, a stable, proper, $m \times m$ minimum phase realization which could be easily constructed from passive elements.

In view of the previous theory, the design strategy to be adopted here will be to adjust the inner loop $\boldsymbol{k}(s)$ and $\boldsymbol{h}(s)$ vectors to provide 'well behaved' dynamic conditions. Thereafter, with the pre-compensator $\mathbf{P}$, configured to produce acceptable steady-state output coupling, the outer loop feedback gain f becomes the ultimate design parameter enabling final dynamic and disturbance suppression characteristics to be achieved.

3 INNER LOOP ANALYSIS

The Laplace transformed open-loop system, given by equation (1), where the system model $\mathbf{G}(s)$ is assumed to be an $m \times m$ linear, regular, proper, or strictly proper realization, admits a factorization

$$\mathbf{G}(s) = \mathbf{L}(s)\frac{\mathbf{A}(s)}{d(s)}\mathbf{R}(s)\mathbf{\Gamma}(s) \quad (10)$$

where $\mathbf{L}(s)$, $\mathbf{A}(s)$, $\mathbf{R}(s)$, $\mathbf{\Gamma}(s)$, and the elements of

$$\frac{\mathbf{A}(s)}{d(s)} \in H_\infty, \quad s \in \mathbb{C}$$

In equation (10), $\mathbf{L}(s)$ contains the left (row) factors, $\mathbf{R}(s)$ contains the right (column) factors, and $\mathbf{\Gamma}(s)$ contains the transformed, actuator finite time delays of $\mathbf{G}(s)$, such that the $m \times m$ matrices comprising (10) are

$$\mathbf{L}(s) = \mathrm{Diag}(\lambda_j(s)/\mathrm{p}_j(s))$$
$$\mathbf{R}(s) = \mathrm{Diag}(\rho_j(s)/\mathrm{q}_j(s))$$
$$\mathbf{\Gamma}(s) = \mathrm{Diag}(\mathrm{e}^{-s\mathrm{T}_j}), \quad 1 \leqslant \mathrm{j} \leqslant \mathrm{m}$$

and $\mathbf{A}(s)$ is a non-singular matrix of rational functions, such that $\det \mathbf{A}(s) \neq 0$, with elements

$$a_{ij}(s) = a_{ij}s^{m-1} + b_{ij}s^{m-2} + \ldots + \gamma_{ij} \quad 1 \leqslant i, j \leqslant m \quad 11$$

As the transformed input-output-disturbance relationship is

$$\boldsymbol{y}(s) = \mathbf{G}(s)\boldsymbol{u}(s) + \boldsymbol{\delta}(s) \quad (12)$$

and if the inner-loop control law is

$$\boldsymbol{u}(s) = \boldsymbol{k}(s)[\bar{r}(s) - \boldsymbol{h}(s)\boldsymbol{y}(s)] \quad (13)$$

then, combining equations (12) and (13) yields

$$\boldsymbol{y}(s) = (\mathbf{I}_m + \mathbf{G}(s)\boldsymbol{k}(s) >< \boldsymbol{h}(s))^{-1}(\mathbf{G}(s)\boldsymbol{k}(s)\bar{r}(s) + \boldsymbol{\delta}(s)) \quad (14)$$

The finite time delays in $\mathbf{\Gamma}(s)$ may be ordered with $\mathrm{T}_i \geqslant \mathrm{T}_j$, $1 \leqslant j \leqslant m$, $i \neq j$, so that the forward path gain vector can be arranged as

$$\boldsymbol{k}(s) = \left[k_1(s)\mathrm{e}^{-s(\mathrm{T}_i-\mathrm{T}_1)}, k_2(s)\mathrm{e}^{-s(\mathrm{T}_i-\mathrm{T}_2)}, \ldots, k_i(s), \ldots, k_m(s)\mathrm{e}^{-s(\mathrm{T}_i-\mathrm{T}_m)}\right]^{\mathrm{T}} \quad (15)$$

Because

$$\boldsymbol{h}(s) = (h_1(s), h_2(s), \ldots, \mathrm{h}_m(s)) \quad (16)$$

and if

$$k_j(s) = k_j\phi_j(s) \quad \text{and} \quad h_j(s) = h_j\chi_j(s) \quad 1 \leqslant j \leqslant m$$

where $\phi_j(s)$ and $\chi_j(s)$ are proper or strictly proper, stable, realizable, minimum phase functions, then they may be selected such that equation (14) becomes

$$\boldsymbol{y}(s) = \left(\mathbf{I}_m + \mathrm{e}^{-sT_i} n(s)\mathbf{L}(s)\frac{\mathbf{A}(s)}{d(s)}\boldsymbol{k}(s) >< \boldsymbol{h}(s)\right)^{-1} \times \left(n(s)\mathbf{L}(s)\frac{\mathbf{A}(s)}{d(s)}\boldsymbol{k}\mathrm{e}^{-sT_i}\boldsymbol{r}(s) + \boldsymbol{\delta}(s)\right) \tag{17}$$

where

$$\boldsymbol{k} = (\mathrm{k}_1, \mathrm{k}_2, \ldots, \mathrm{k}_m)^{\mathrm{T}} \tag{18}$$

and

$$\boldsymbol{h} = (\mathrm{h}_1, \mathrm{h}_2, \ldots, \mathrm{h}_m) \tag{19}$$

$$d(s) = s^{\kappa} + a_1 s^{\kappa-1} + \cdots + a_0$$

and

$$\deg(n(s)a_{i,j}(s)) < \kappa \quad 1 \leqslant i,\ j \leqslant m$$

The determinant required in equation (17) is

$$\det\left[\mathbf{I}_m + \mathrm{e}^{-sT_i} n(s)\mathbf{L}(s)\frac{\mathbf{A}(s)}{d(s)}\boldsymbol{k}(s) >< \boldsymbol{h}(s)\right] = 1 + \mathrm{e}^{-s_i} n(s) < \boldsymbol{h}\frac{\mathbf{A}(s)}{d(s)}\boldsymbol{k} > \tag{20}$$

The inner product in equation (20) may be expressed as

$$< \boldsymbol{h}\mathbf{A}(s)\boldsymbol{k} > = \left[1, s, \ldots, s^{m-1}\right]\begin{bmatrix} \gamma_{11} & \gamma_{12} & \cdots & \gamma_{mm} \\ \vdots & \vdots & & \vdots \\ b_{11} & b_{12} & \cdots & b_{mm} \\ a_{11} & a_{12} & \cdots & a_{mm} \end{bmatrix} \times \begin{bmatrix} \mathrm{k}_1\mathrm{h}_1 \\ \mathrm{k}_2\mathrm{h}_1 \\ \vdots \\ \mathrm{k}_m\mathrm{h}_m \end{bmatrix} \tag{21}$$

If in equation (21) the gain ratios are

$$\mathrm{k}_2 = \mathrm{n}_1\mathrm{k}_1, \quad \mathrm{k}_3 = \mathrm{n}_2\mathrm{k}_1, \ldots, \quad \mathrm{k}_m = n_{m-1}\mathrm{k}_1 \tag{22}$$

and

$$< \boldsymbol{h}\mathbf{A}(s)\boldsymbol{k} > = b(s) \tag{23}$$

then equation (23) implies that

$$\mathrm{k}_1[\mathbf{Q}]\boldsymbol{h} = (b_{m-1}, b_{m-2}, \ldots, b_0)^{\mathrm{T}} \tag{24}$$

where

$$\mathbf{Q} = \begin{bmatrix} \gamma_{11} + \gamma_{12}n_1 + \cdots + \gamma_{1m}n_{m-1} & \gamma_{21} + \gamma_{22}n_1 + \cdots + \gamma_{2m}n_{m-1} & \cdots & \gamma_{m1} + \gamma_{m2}n_1 + \cdots + \gamma_{mm}n_{m-1} \\ \vdots & \vdots & & \vdots \\ b_{11} + b_{12}n_1 + \cdots + b_{1m}n_{m-1} & b_{21} + b_{22}n_1 + \cdots + b_{2m}n_{m-1} & \cdots & b_{m1} + b_{m2}n_1 + \cdots + a_{mm}n_{m-1} \\ a_{11} + a_{12}n_1 + \cdots + a_{1m}n_{m-1} & a_{21} + a_{22}n_1 + \cdots + a_{2m}n_{m-1} & \cdots & a_{m1} + a_{m2}n_1 + \cdots + a_{mm}n_{m-1} \end{bmatrix}$$

and b_j, $0 \leqslant j \leqslant m-1$, are the coefficients of $b(s)$, given in equation (23). Providing the weak constraint, that n_1, $n_2, \ldots,$ n_{m-1} can be selected in equation (24) so that the matrix is invertible, then a unique solution for $(\mathrm{h}_1, \mathrm{h}_2, \ldots, \mathrm{h}_m)\mathrm{k}_1$ exists.

Following the choice of a suitable $b(s)$ function and the gain ratios $n_1, n_2, \ldots, n_{m-1}$, the closed-loop dynamics arising from equation (17) are fully defined. If equation (24) is solved, then the measurement vector $\boldsymbol{h}$ can be evaluated once an arbitrary value for k_1 has been decided upon. Note that the inner-loop design procedure is equally valid for non-square system models.

4 OPTIMIZATION

Now that a route for designing closed-loop systems, using the transfer function matrix and output measurements alone has been established, the possibility of optimizing this process can be considered. An indication that the freedom exists to do this arises from the arbitrary choice of n_1, n_2 etc. for the gain ratios.

Detecting the absolute minimum control effort required, for disturbance suppression, under closed-loop conditions, with the constraint that the controller model generates a particular polynomial, would provide a useful, initial benchmark. This polynomial influences the migration pattern of the closed-loop poles so that control effort minimization to disturbances and the desired inner-loop system response to input changes could be achieved simultaneously. The controller equation for a system having m inputs and m outputs is given by equation (2).

The control effort at time t is proportional to

$$(|k_1h_1| + |k_2h_1| \cdots |k_mh_1|)|y_1(t)| + (|k_1h_2| + \cdots + |k_mh_2|)|y_2(t)| + \cdots + (|k_1h_m| + |k_2h_m| + \cdots + |k_mh_m|)|y_m(t)|$$

Hence, the control energy costs, under these conditions, are proportional to

$$E(t) = \int_{t=0}^{t=T_f} \left(\sum_{i=1}^{m} k_i^2 \sum_{j=1}^{m} h_j^2 y_j^2(t) \right) dt \tag{25}$$

then for arbitrary changes in the transformed output vector $\boldsymbol{y}(t)$, following arbitrary disturbance changes

$$J = \sum_{i=1}^{m} k_i^2 \sum_{j=1}^{m} h_j^2 \tag{26}$$

would minimize the control energy required, given by expression (25). If the relationships

$$k_2 = n_1 k_1, \quad k_3 = n_2 k_1, \; \ldots, \quad k_m = n_{m-1} k_1$$

are adopted, then equation (26) can be written as

$$J = (k_1)^2 (1 + n_1^2 + n_2^2 + \cdots + n_{m-1}^2) \times (h_1^2 + h_2^2 + \cdots + h_m^2) \tag{27}$$

and $h_1^2 + h_2^2 + \cdots + h_m^2 <\boldsymbol{h}, \boldsymbol{h}>$. The closed-loop determinant is given by equation (20) with the inner product equated to $b(s)$, as in equation (23) then from equation (24)

$$\boldsymbol{h} = k_1^{-1} \mathbf{Q}^{-1} \boldsymbol{b} \tag{28}$$

Upon substituting for $\boldsymbol{h}$ from equation (28), equation (27) becomes

$$J = (1 + n_1^2 + n_2^2 + \cdots + n_{m-1}^2) \boldsymbol{b}^{\mathrm{T}} (\mathbf{Q}^{-1})^{\mathrm{T}} \mathbf{Q}^{-1} \boldsymbol{b} \tag{29}$$

To find the minimum value for J, assuming, for example, that $m = 3$ gives

$$J = (1 + n_1^2 + n_2^2) \boldsymbol{b}^{\mathrm{T}} (\mathbf{Q}^{-1})^{\mathrm{T}} \mathbf{Q}^{-1} \boldsymbol{b}$$

where J is minimized when

$$\frac{\partial J}{\partial n_1} = 0, \; \frac{\partial J}{\partial n_2} = 0, \quad \text{and}$$

$$\frac{\partial^2 J}{\partial n_1^2} \frac{\partial^2 J}{\partial n_2^2} - \left(\frac{\partial^2 J}{\partial n_1 \partial n_2} \right)^2 > 0, \quad \text{if } \frac{\partial^2 J}{\partial n_1^2} > 0$$

For $m > 3$, a numerical optimization routine could be employed to establish the values of $n_1, n_2, \ldots, n_{m-1}$ which minimize J. There are many procedures available for this task, as indicated by Bunday [**6**], with rapid convergence and high accuracy characteristics.

This completes the inner-loop analysis.

The employment of the inner-loop configuration and an absolute, minimum effort controller while attaining a particular closed-loop pole pattern would not, in general, achieve specified, steady-state disturbance recovery conditions. However, the disturbance recovery transient would, of course, be determined by this pole configuration.

To achieve the steady-state, disturbance offset condition required, the outer-loop feedback gain f could be adjusted by increasing $0 < f < 1.0$, as indicated by equation (6). This would perturb the system's transient behaviour and recognition of this should be exercized by aiming for modest response improvements arising from the inner-loop dynamics.

Thereafter, the control effort required would become the relative minimum effort, commensurate with the achievement of particular steady-state disturbance suppression characteristics. As shown by equation (56), increasing f from zero is instrumental in increasing $\boldsymbol{k}(s) >< \boldsymbol{h}(s)$ to $\boldsymbol{k}(s) >< \boldsymbol{h}(s) / (1 - f)$. This is equivalent to increasing b_0 of equation (24) to $b_0/(1 - f)$, thereby elongating and elevating the performance index J curve, so that $J_{\min}$ is moved upwards while retaining the original, optimum, minimum effort gain ratio values of $n_1, n_2, \ldots, n_{m-1}$. The obvious conclusion from this is that, in the absence of all other inputs, the control effort expended is devoted entirely to the disturbance suppression and recovery. Consequently, the performance index J, being proportional to the control effort, is also a direct measure of this condition.

In aiming for the minimum J, for a given pole configuration, the disturbance recovery transient is executed with maximum energy efficiency. By closing the outer-loop, upon increasing f from zero, the system's closed-loop disturbance suppression characteristics would be enhanced while perturbing the closed-loop pole pattern. The $S(i\omega)$ curves would not be significantly altered by prudent adjustment and the optimum performance, and low frequency disturbance containment prevails.

5 DISTURBANCE REJECTION ANALYSIS

It is apparent from equation (22) that there will be many values of n_j, $1 \leqslant j \leqslant m-1$ which could be selected while satisfying equation (24). However, choosing these gain ratios arbitrarily affects the robustness of the feedback configuration to parameter changes, the control energy dissipation, and disturbance rejection properties of the system.

For complete steady-state, low frequency disturbance suppression, integral action would generally be required and the availability of infinite feedback control effort if integral 'wind up' is to be avoided. In practice, some form of approximate integration over a limited frequency range, such as phase lag compensation, is usually employed. Otherwise, to confine output excursions to disturbances, the maximum proportional feedback gain, commensurate with acceptable transient conditions and modelling/parameter uncertainties, may be employed.

In the following, bounds on the disturbance response arising from changes in the sensitivity matrix are determined. Gain ratios for which there are rapid changes in the performance index J and hence in disturbance containment, also become apparent. These values indicate a lack of robustness to modelling variations and should be avoided.

In many multi-body electro-mechanical systems, the only continuously perturbed signals entering the system, arise from changes in $\boldsymbol{\delta}(s)$ so that with $\mathbf{r}(s) = 0$, equation (6) becomes

$$\boldsymbol{y}(s) = S(s)\boldsymbol{\delta}(s) \tag{30}$$

where

$$S(s) = (\mathbf{I}_m + \mathbf{G}(s)(\boldsymbol{k}(s) >< \boldsymbol{h}(s) + \mathbf{PF}))^{-1}$$

The sensitivity matrix $\mathbf{S}(s)$ in equation (30) should be such that changes in $\boldsymbol{\delta}(s)$ result in acceptable changes in $\boldsymbol{y}(s)$. These output excursions arise from relatively low frequency variations in $\boldsymbol{\delta}(s)$, as discussed by Skogestad and Postlethwaite [7]. Moreover, since, for physically realizable, electro-mechanical systems, $\mathbf{G}(s)$ must be strictly proper, the closed-loop system provides no attenuation at high frequencies as $\mathbf{S}(s) \to \mathbf{I}_m$.

Consequently, the adjustment of the steady-state system disturbance suppression properties, by increasing f in equation (30), would ensure enhanced attenuation following 'low frequency' perturbations. Moreover, for increasing values of frequency, the singular values of $\mathbf{S}(s)$ should be smooth, differentiable, and almost monotonic curves, providing a prudent policy of regulation is pursued.

The attenuation secured by the system lies between the lower and upper singular values of the $\mathbf{S}(s)$ matrix, as shown by Zames [8].

Specifically

$$\underline{\lambda}(\mathbf{S}(s)) \leqslant \frac{\|\boldsymbol{y}(s)\|_2}{\|\boldsymbol{\delta}(s)\|_2} \leqslant \bar{\lambda}(\mathbf{S}(s)) \tag{31}$$

where $\underline{\lambda}(\mathbf{S}(s))$ and $\bar{\lambda}(\mathbf{S}(s))$ are the smallest and largest singular value amplitudes of $\mathbf{S}(s)$, respectively, and $\|\bullet\|_2$ denotes the Euclidean norm, $s = i\omega$, $0 \leqslant \omega \leqslant \infty$, of $\boldsymbol{y}(s)$ and $\boldsymbol{\delta}(s)$, respectively.

It is also apparent from equation (31) that providing the upper bound $\bar{\lambda}(\mathbf{S}(s)) \leq 3$ dB, $s = i\omega$, $0 \leqslant \omega \leqslant \infty$, the system will be stable with a maximum 'high' frequency resonant peak $\leqslant 1.4$, $\|\boldsymbol{\delta}(s)\|_2 \neq 0$, once the closed-loop outputs are substantially decoupled.

The singular values of the low frequency sensitivity matrix, given in equation (6), can be computed in the frequency domain for $f = 0$, from

$$\det[\mathbf{I}_m\lambda^* - (\mathbf{I}_m + \mathbf{G}(s)(\boldsymbol{k}(s) >< \boldsymbol{h}(s)))^{-1}]_{s=i\omega} = 0$$

The steady-state singular values may be estimated from

$$\det[\mathbf{I}_m\lambda^* - (\mathbf{I}_m + \mathbf{G}(0)(\boldsymbol{k}(0) >< \boldsymbol{h}(0)))^{-1}] = 0$$

as

$$\mathbf{G}(0)\boldsymbol{k}(0) >< \boldsymbol{h}(0)$$

has m singular values of

$$\gamma_1 = \gamma_2 = \cdots \gamma_{m-1} = 0 \quad \text{and} \quad \gamma_m = \sum_{j=1}^{m} \bar{k}_j h_j$$

where

$$\bar{\boldsymbol{k}} = \mathbf{G}(0)\boldsymbol{k}(0) \tag{33}$$

Consequently, it is easy to show that the singular values, λ_i^*, $1 \leqslant i \leqslant m$, of equation (32) are

$$\lambda_1^* = \lambda_2^* = \cdots \lambda_{m-1}^* = 1 \quad \text{and}$$
$$\lambda_m^* = \frac{1}{1 + \sum_{j=1}^{m} \bar{k}_j h_j(0)} \tag{34}$$

where $\bar{k}_j$ is the j^{th} element of $\bar{\boldsymbol{k}}$.

As shown by equation (6), $\mathbf{S}(s) = (1-f)\ (\mathbf{I}_m + \mathbf{G}(s)\ \boldsymbol{k}(s) >< \boldsymbol{h}(s))^{-1}$, so that the low frequency singular value amplitudes of $\mathbf{S}(s)$ are reduced to λ_j where

$$\lambda_j = (1-f)\lambda_j^*, \quad 1 \leqslant j \leqslant m,\ 0 < f < 1 \tag{35}$$

Consequently, the bound on the low frequency attenuation properties of the system becomes

$$\underline{\lambda}(\mathbf{S}(0)) \leqslant \frac{\|y(0)\|_2}{\|\delta(0)\|_2} \leqslant \bar{\lambda}(\mathbf{S}(0)) \tag{36}$$

The estimate from equation (36) is conservative. An accurate measure of the low frequency disturbance attenuation properties of the system can be easily computed from the direct evaluation of equation (30). In this regard if

$$\bar{s}(\mathbf{S}(0)) = \text{largest element of } \mathbf{S}(0)$$
$$\underline{s}(\mathbf{S}(0)) = \text{smallest element of } \mathbf{S}(0)$$

then

$$\underline{s}(\mathbf{S}(0)) \leqslant \frac{\|y(0)\|_2}{\|\delta(0)\|_2} \leqslant \bar{s}(\mathbf{S}(0))$$

provides an improved, low frequency attenuation bound.

6 STABILITY OF COMBINED SYSTEM

The input-output relationship for the complete closed-loop system is given by equation (5). Consequently, the input-output stability condition is dependent on the denominator of this equation.

If, for the sake of simplicity, the outer-loop feedback gain matrix **F** is given by

$$\mathbf{F} = \mathrm{Diag}(f_1, f_2, \ldots, f_m)$$

and if once again

$$f_1, f_2, \ldots, f_m = f$$

then the denominator of equation (5) may be calculated from

$$\det\left\{\mathbf{I}_m + \mathbf{G}(s)\left[\frac{\boldsymbol{k}(s) >< \boldsymbol{h}(s)}{(1-f)} + \frac{\mathbf{G}(0)^{-1}f}{(1-f)}\right]\right\}$$

From this expression, it is evident that the elements of the feedback-compensator matrix

$$\left[\frac{\boldsymbol{k}(s) >< \boldsymbol{h}(s)}{(1-f)} + \frac{\mathbf{G}(0)^{-1}f}{(1-f)}\right]$$

become infinite as $f \to 1$. In practice, this would always result in closed-loop system instability.

For values of $f \leqslant 0.5$, the inner-loop feedback gain is amplified while the effect of the outer loop, arising from $\mathbf{G}(0)^{-1}f/(1-f)$, is attenuated. Once, $0.5 < f < 1.0$, both the inner- and outer-loop gains are effectively amplified with $f/(1-f)$ and $1/(1-f)$ approaching infinity.

Essentially, amplifying $\boldsymbol{k}(s) >< \boldsymbol{h}(s)$ by $1/(1-f)$ $f < 1$ is equivalent, as stated earlier, to multiplying b_o in equation (24) by this amount. Consequently, the absolute minimum value of J, achieved initially, from the optimization process is increased by the use of the outer-loop feedback to $J/(1-f)$, while the gain ratio remains unchanged at n, with $\boldsymbol{k}$ becoming $(1,\ n)^{\mathrm{T}}/(1-f)$, $m = 2$. Owing to these factors, the system's disturbance suppression properties are enhanced.

Hence, by setting the inner-loop frequency response or characteristic equation zero pattern, such that the amplification of $\boldsymbol{k}(s) >< \boldsymbol{h}(s)$ to $\boldsymbol{k}(s) >< \boldsymbol{h}(s)/(1-f)$ can be safely accommodated, dynamic recovery, and steady-state disturbance rejection can be adjusted, using the outer-loop feedback gain f.

Confirmation of the relative stability for the closed-loop system can be easily computed using the characteristic locus method, presented by Macfarlane [9]. This is evident from the establishment of the pre- and feedback compensators in equations (8) and (9) and hence, the conventional multivariable feedback structure, indicated by equation (7).